FUNCTIONAL ROLE OF THE CONSERVED AMINO ACIDS CYSTEINE 81, ARGININE 279, GLYCINE 280 AND ARGININE 283 IN ELONGATION FACTOR TU FROM *ESCHERICHIA COLI*

Fan Mo

B. Sc. University of Lethbridge, 2008

A Thesis

Submitted to the School of Graduate Studies

of the University of Lethbridge

in Partial Fulfilment of the

Requirements for the Degree

MASTER of SCIENCE

Department of Chemistry and Biochemistry

University of Lethbridge

LETHBRIDGE, ALBERTA, CANADA

Abstract

During protein synthesis, elongation factor Tu (EF-Tu) delivers aminoacyl-tRNA (aa-tRNA) to the A-site of mRNA-programmed ribosomes in a GTP-dependent manner. To enable future studies on the functional and structural requirement of EF-Tu's function, a Cysteine-free variant of EF-Tu was constructed suitable for subsequent labelling of the protein and use in kinetic studies. Here, the kinetic properties of three Cysteine-less EF-Tu variants are reported, demonstrating that only the variant with the Alanine substitution in position 81 retains wild-type activity with respect to the interaction with guanine nucleotides, aa-tRNA and the ribosome. To explore a possible tRNA independent pathway for the GTPase activation signal, three residues in domain II of EF-Tu (Arginine 279, Glycine 280, Arginine 283) were mutated; the activity of EF-Tu variants were analyzed. Results suggest that these residues are indeed required for efficient ribosome-dependent stimulation of the GTPase activity of EF-Tu.

Acknowledgement

I would like to thank my supervisor Dr. Hans-Joachim Wieden for the opportunity to learn, work and teach in the lab and his guidance through these years.

I also want to thank all my committee members and specially Dr. Ute Kothe for all valuable suggestions and support during my study.

Thank you to all the Wieden and Kothe lab members, who not only are my coworkers but also my friends, and even sometimes like family.

Last, I really would like to thank my family for all their supports. I especially want to thank my parents who allowed and supported me to study abroad, and encouraged me to move on.

Table of Contents

List of Figures

List of Tables

List of Abbreviations

aaRS	aminoacyl-transfer ribonucleic acid synthetase
aa-tRNA	aminoacyl-transfer ribonucleic acid
AMP	adenosine monophosphate
ASL	anticodon stem-loop
ATP	adenosine triphosphate
bp	base pair
cryo-EM	cryo-electron microscopy
DNA	deoxyribonucleic acid
DTT	dithiothreitol
E. coli	*Escherichia coli*
EDTA	ethylenediaminetetraacetic acid
EF-G	elongation factor G
EF-Ts	elongation factor Ts
EF-Tu	elongation factor Tu
fMet	formylmethionine
FRET	fluorescence resonance energy transfer
GDI	guanine nucleotide dissociation inhibitor
GDP	guanosine diphosphate
GEF	guanine nucleotide exchange factor
GTP	guanosine triphosphate
HPLC	high-pressure liquid chromatography
IF	initiation factor
IPTG	isopropyl β-D-1thiogalactopyranoside
mant	2'-(or -3')-*O*-(*N*-methylanthraniloul)
mRNA	messenger ribonucleic acid
MWCO	molecular weight cut off

K_D	equilibrium dissociation constant
OAc	acetate
OD	optical density
PDB	Protein Data Bank
PEP	phosphoenolpyruvate
P_i	inorganic phosphate
PK	pyruvate kinase
PMSF	phenylmethylsulfonylfluoride
PTC	peptidyl transferase center
RF	release factor
RNA	ribonucleic acid
RNase	ribonuclease
RRF	ribosome recycling factor
SD	Shine-Dalgarno
SDS-PAGE	sodium dodecyl sulphate polyacrylamide gel electrophoresis
SEC	size exclusion chromatography
SRL	sarcin-ricin loop
rRNA	ribosomal ribonucleic acid
TFA	trifluoroacetic acid
T. thermophilus	*Thermus thermophilus*
tRNA	transfer ribonucleic acid
TLC	thin layer chromatography
TPCK	*N*-tosyl-L-phenylalanyl chloromethane
UTR	untranslated region

Chapter 1 Introduction

1.1 Overview of translation

The central dogma of molecular biology as called by Francis Crick describes the relationship between deoxyribonucleic acid (DNA), ribonucleic acid (RNA) and protein. DNA directs its replication and transcription to RNA, and RNA directs its translation to proteins. Although the chemistry behind peptide bond formation is relatively simple, the process to convert genetic information from the mRNA to a functional protein is quite complex. This process is carried out by a large macromolecular complex called the ribosome and involves the precise coordination and timing of a large number of molecules, in order to accurately select from the 20 different amino acids in the order that is specific to a particular mRNA.

1.1.1 tRNA

Crick first hypothesised that an adaptor molecule, now known as "transfer RNA" (tRNA), carries a specific amino acid and recognizes the corresponding codon, and that the adaptor would contain RNA which then could through complementary base pairing interact with the messenger RNA (mRNA) facilitating codon recognition (Crick 1966). Later on, the discovery of the existence of tRNA confirmed Crick's adaptor hypothesis, and suggested base pairing between a trinucleotide anticodon and the mRNA codon (Hoagland *et al.* 1958; Shapiro *et al.* 1965).

The tRNA consists of ~76 nucleotides and forms a cloverleaf-shaped secondary structure (Holley *et al.* 1965) (Figure 1.1). To date, sequences from more than 4,000 tRNAs from over 200 organisms are known, which all share seven basic structural features: (1) a 5'-end phosphate group, (2) a 7 base pair (bp) stem formed by Watson-

Crick base pairing, known as the acceptor stem, (3) a 3 to 4 bp stem with a loop containing the modified base dihydrouridine; and that is designated as the D loop, (4) anticodon arm, a 5 bp stem connecting a loop containing the bases of the triplet anticodon, which is complementary to the codon specific to the respective tRNA, (5) the variable arm, termed due to the variability of number and type of nucleotides appearing at these positions, (6) a 5 bp stem with a loop containing the conserved TψC sequence (ψ, pseudouiridine), known as the T arm or the TψC arm, and (7) a 3'-end formed by a CCA sequence with a 3'–OH group.

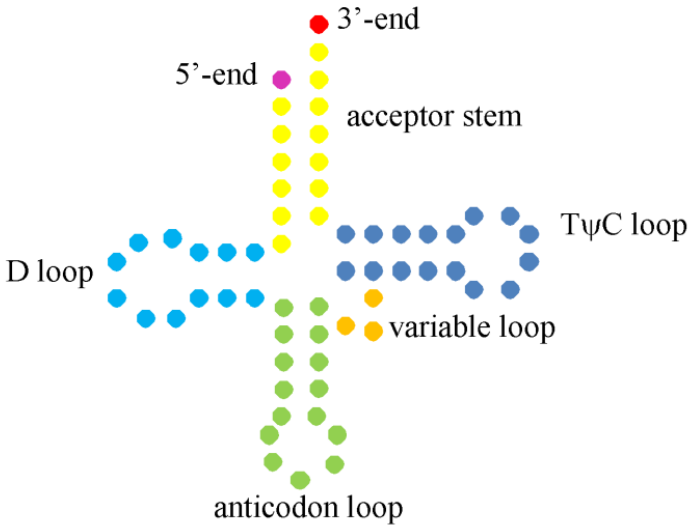

Figure 1.1 Cloverleaf structure of tRNA. The 5'-terminus is shown in magenta, the acceptor stem is yellow, the D loop is cyan, the anticodon loop is green, the variable arm is orange, the TψC arm is blue, and the 3'-end is shown in red.

The crystal structure of yeast $tRNA^{Phe}$ revealed that an L-shaped molecule is formed from two RNA double helical "legs", one containing the acceptor stem and the T loop and the other contains the D and the anticodon loop (Sussman *et al.* 1978) (Figure

1.2). Both legs of the tRNA molecule are around 60 Å long, while the anticodon and amino acid acceptor stem is well separated around 76 Å apart at the two opposite ends of the molecule. The structure of the tRNA is stabilized by a number of intramolecular interactions. Typically 71 of 76 bases in yeast $tRNA^{Phe}$ are involved in stacking interaction. Therefore, most of the bases are protected from interaction with solvent molecules. However, due to their specific biological function, anticodon bases and the CCA 3'-end remain exposed to the solvent.

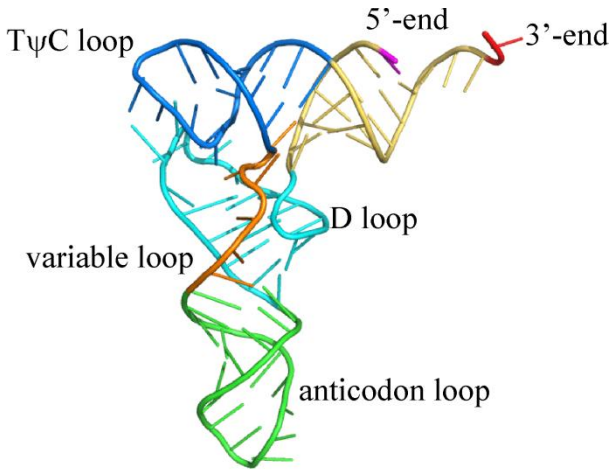

Figure 1.2 X-ray structure of yeast $tRNA^{Phe}$. The conserved L-shape of the tRNA molecule is shown as cartoon representation (generated with PyMol). The 3'-end is coloured red, the acceptor stem is yellow, the TψC loop is blue, the variable loop is orange, the anticodon loop is green, the D loop is cyan, and the 5'-end is magenta. (PDB: 6TNA)

The aminoacyl-tRNA synthetases (aaRSs) are a family of enzymes that ensure that the correct amino acid is covalently attached to its cognate tRNA, and are responsible for the production of the charged tRNAs that are required for translating mRNAs into functional proteins. In order to attach an amino acid to the 3'-end of its cognate tRNA forming the aminoacyl-tRNA (aa-tRNA), the amino acid first reacts with

ATP to form an activated aminoacyl-adenylate. Then the activated amino acid is transferred to the tRNA to form aminoacyl-tRNA and AMP (Delarue 1995). Although in cells different aaRSs are responsible for different amino acids, these aaRSs can be divided into two different classes (I and II), each containing 10 members. Previous studies have shown that in general Class I aaRSs recognize their cognate tRNA through anticodon recognition, while Class II aaRSs recognize the acceptor stem. Interestingly, Class I aaRSs aminoacylate the tRNA at 2'–OH group of the 3'-end, but Class II aaRSs aminoacylate at the 3'–OH group. Moreover, Class I aaRSs tend to activate larger and more hydrophobic amino acids than Class II aaRSs (Cavarelli and Moras 1993). The error rate of aaRSs is about 1 in 10,000. This is a remarkable number as many aaRSs face the challenge to discriminate between structurally very similar amino acids. To achieve this level of accuracy, the aaRSs have adopted a double-sieve mechanism, which requires an additional proofreading or editing step that occurs at a specific catalytic site in the enzyme, known as the editing domain. The editing step can occur before or after aminoacylation with the correct amino acid (Banerjee *et al.* 2010), and utilizes the conformational change of the 3'-end of the tRNA to switch between synthetic and editing modes. However, the exact mechanism is unclear (Ling *et al.* 2009). Once aa-tRNA is released from aaRS, it will be delivered to the translating ribosome by elongation factor (EF)-Tu.

1.1.2 The Ribosome

In translation, the mRNA-directed polypeptide synthesis takes place on the ribosome. The movement of tRNA and mRNA through the ribosome is a complicated process that requires both high speed and high accuracy. The ribosome has been first

visualized in the late 1930s by Albert Claude using dark-field microscopy, and was named after its main components: RNA and protein. In all organisms, the ribosome consists of two subunits (Figure 1.3). In *Escherichia coli*, the 50S large subunit contains 2 RNAs (5S and 23S rRNA) and 31 different proteins, while the 30S small subunit contains the 16S rRNA and 21 different proteins. Interestingly, 66% of the ribosomal mass is contributed by rRNAs, and only 34% by proteins in bacteria. *In vivo* studies of the ribosomal assembly process suggest that the main event is rRNA processing (Nierhaus 1991). There are two processes involved in the production of mature rRNA: (1) trimming of the rRNAs to the mature molecules, and (2) chemical modification of the rRNAs. A number of enzymes participate in the events that cleave pre-rRNA into mature rRNA, such as RNase III, RNase P, M16 and M5 (Srivastava and Schlessinger 1990). Although, both 16S and 23S rRNA are methylated and pseudouiridylated during ribosomal assembly, the function of the modifications is unknown. Ribosome assembly not only requires the correct processing of rRNAs, but also the proteins and their sequential binding. *In vitro* studies have shown that the 50S ribosome can successfully reconstitution from its components. However, it is an extremely slow process (*in vivo*: a few minutes at 37^{o}C; *in vitro*, 90 min at 50^{o}C) (Nierhaus 1991).

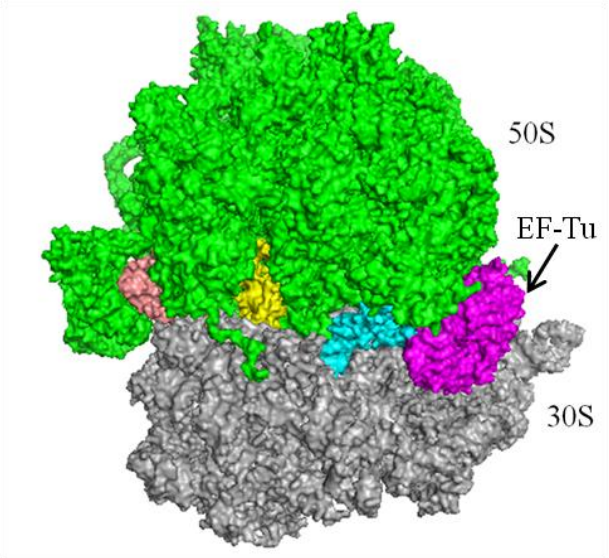

Figure 1.3 Structure of the 70S ribosome from *Thermus thermophilus* in complex with EF-Tu. 50S ribosomal subunit is shown in green, 30S ribosomal subunit is in grey. EF-Tu is magenta, A-site tRNA is blue, P-site tRNA is yellow and E-site tRNA is salmon. (PDB: 3FIN and 3FIC)

The first high resolution structure of a ribosomal subunit was published by Ban *et al.* with a resolution of 2.4 Å from the archaean *Haloarcula marismortuii* (Ban *et al.* 2000). The structure only contained the 50S subunit, and the ribosomal proteins L1, L7/L12 stalks, and L11-RNA region which are functionally important for factor binding and translocation, as well as some stem loops of the RNA involved in contacts with the 30S subunit were disordered (Ramakrishnan 2002). Nonetheless, this is the first structure to show that water molecules and metal ions are also involved in the coordination of ribosomal structure. With the dramatic improvement of the cryo-electron microscopy (cryo-EM) technique, more and more medium resolution structures of the ribosome in complex with different factors have been solved, and allowed a detailed study of the structural and functional mechanism of translation.

The *E. coli* 50S ribosomal subunit has a molecular weight of 1,590 kDa, 70% of its weight is contributed by the 2,904 nucleotide long 23S rRNA and the 120 nucleotide of the 5S rRNA. The remaining 30% arise from 31 proteins. It has been shown that the rRNAs cooperatively interact with proteins during subunit assembly (Figure 1.4). Protein L5 and L18 have been shown to be essential for the association of the 5S and 23S rRNAs into a complex that contains equimolar amounts of all four components. The integration of 5S rRNA into this complex induces a conformational change in the 23S rRNA (Spierer *et al.* 1979). Protein L2 has been shown to interact with the central segment of the 23S rRNA; and the associations of L5, L10/11, and L28 with the central and 3'-end of the 23S rRNA are depended on the association of the L16, L2 and L1/3/6. Furthermore, the sarcin-ricin loop (SRL), a highly conserved loop in the 23S rRNA, is important for the function of many GTP-dependent protein factors (Hausner *et al.* 1987), while L7/12 stimulates EF-Tu's GTPase activity (Donner *et al.* 1978; Diaconu *et al*. 2005). The ribosomal protein L1 interacts with deacylated tRNA and is involved in tRNA release (Trabuco *et al.* 2010) . In order to facilitate translation, the 23S rRNA forms three functionally distinct tRNA-binding sites: (1) A-site, interacts with newly incoming aa-tRNA; (2) P-site, binding site for peptidyl tRNA, and (3) E-site, where the deacylated tRNA dissociates from the ribosome.

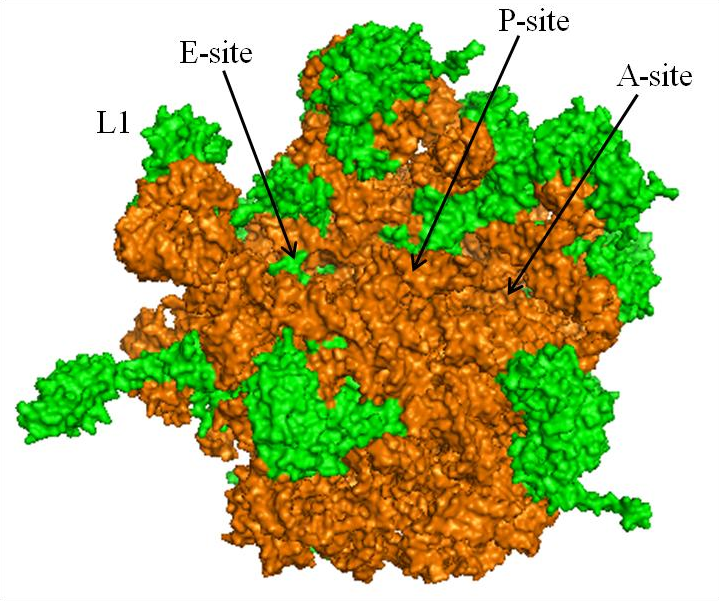

Figure 1.4 50S ribosomal subunit from *Thermus thermophilus* (interface view). 50S ribosomal proteins are shown in green, 23S and 5S rRNA are in orange. (PDB: 3FIN)

Similar to the 50S ribosomal subunit, the *E. coli* 930 kDa 30S subunit consists of a 1,542 nucleotide 16S rRNA with 60% molecular weight and 21 proteins with 40% of the weight (Figure 1.5). Like the 50S subunit, the 30S subunit contains part of the A-site, P-site and E-site for tRNA interaction. However, it is also involved in interacting with the mRNA. The 16S rRNA contains a pyrimidine-rich sequence at the 3'-end, that has been shown to base pair with a purine-rich sequence (Shine-Dalgarno (SD) sequence) of the mRNA, around 10 nucleotides upstream of the start codon (Shine and Dalgarno 1974). The available crystal structures suggest that the Shine-Dalgarno helix is bound to a large cleft between the head and the back of the platform of the 30S subunit (Yusupova *et al.* 2001). S4 and S7 proteins have been shown to be important to initiate folding of 16S rRNA, typically S7 binds to 3'-end of the 16S rRNA and stimulates the binding of other ribosomal proteins to the subunit (Nowotny and Nierhaus 1988). Codon-anticodon

recognition takes place at the 30S subunit A-site, which is the binding site for newly incoming aa-tRNA. X-ray crystal structural studies suggest that the interaction of A1492, A1493, and G530 in the 16S rRNA with the minor groove of the first two codon-anticodon base pairs may stabilize the structure (Selmer *et al.* 2006). On the other hand, the P-site functions by holding the tRNA in position in order to maintain the reading frame, where A1339 and G1338 of the 16S rRNA and nucleotide 790 at the tip of 30S platform interact with the anticodon stem loop of the P-site tRNA, and prevent moving of the tRNA into the E-site (Selmer *et al.* 2006).

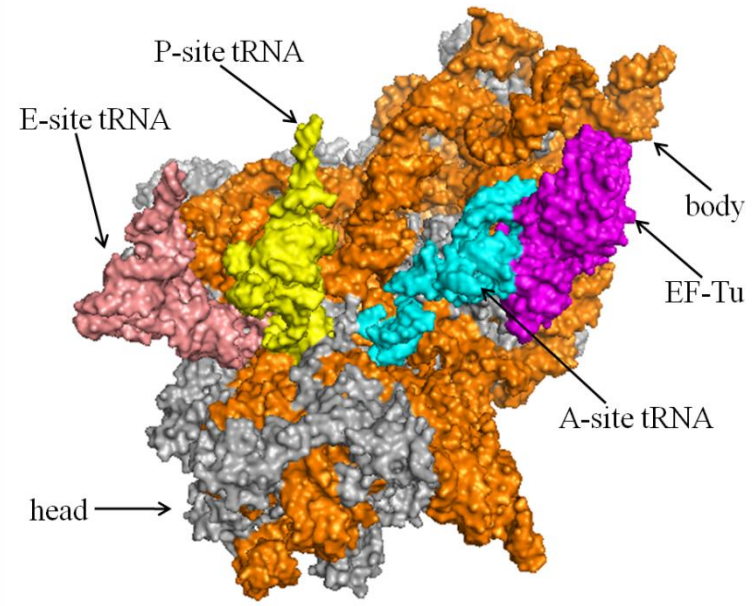

Figure 1.5 30S ribosomal subunit from *Thermus thermophilus* in complex with tRNAs and EF-Tu (solvent view). 30S ribosomal proteins are shown in grey, 16S rRNA in orange, EF-Tu in magenta. The A-site tRNA is coloured in cyan, the P-site tRNA in yellow and the E-site tRNA in salmon. (PDB: 3FIC)

1.2 Initiation

In all living cells, translation can be divided into three processes: initiation, elongation, termination. Several components are required for efficient bacterial

translation initiation: ribosome, aminocylated and formylated initiator tRNA (fMet-tRNA^{fMet}), mRNA, and three initiation factors (IF1, IF2 and IF3) (Figure 1.6).

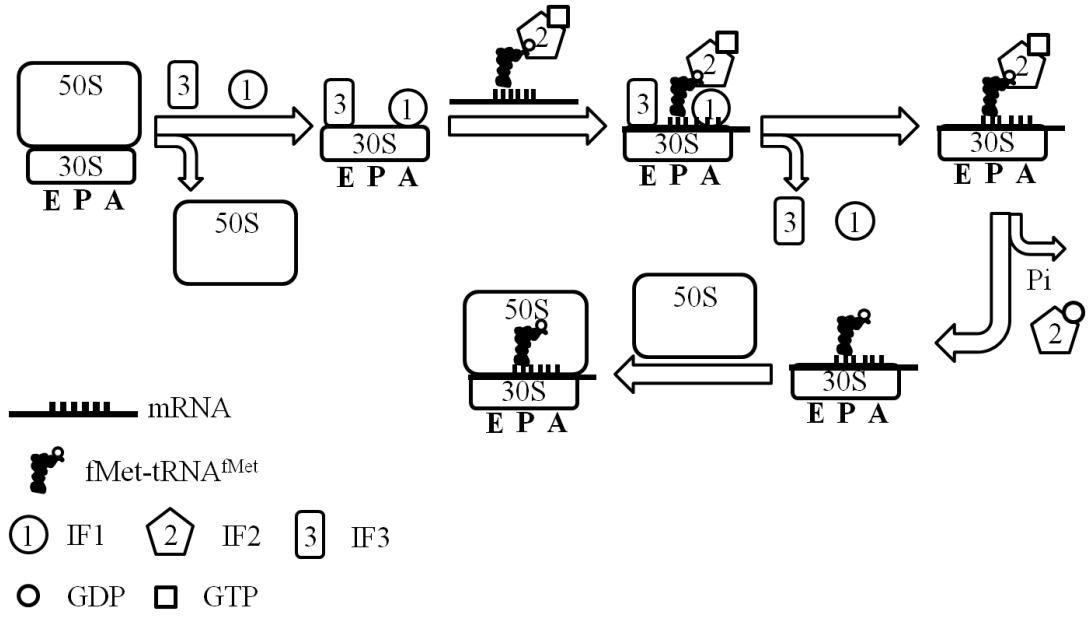

Figure 1.6 Translation initiation pathway in bacteria. Initiation factors are signified by their respective numbers. The binding of IF3 and IF1 to the 70S ribosome induce the dissociation of the two subunits, following the association of mRNA and IF2·GTP·fMet-tRNA^{fMet}, IF1 and IF3 dissociate from the pre-initiation complex. After hydrolysis of GTP, IF2 dissociates, 50S ribosomal subunit re-associates with the 30S subunit and forms the initiation complex.

Translation is initiated by the binding of mRNA to the 30S ribosomal subunit. IF3 has been shown to bind tightly to the 30S subunit to promote the dissociation of the 70S ribosome, and to prevent the re-association of 50S with the 30S subunit (Godefroy-Colburn *et al.* 1975). IF3 is also important for the selection of fMet-tRNA^{fMet} to the P-site by preventing the binding of elongator tRNA (Hartz *et al.* 1990). fMet is the first amino acid of a polypeptide chain and ensures the correct initiation of translation at the translation initiation region of the mRNA. In bacteria, mitochondria and chloroplasts,

methionyl-tRNA (Met-tRNA^{fMet}) is specifically N-formylated by methionyl-tRNA formyltransferase to produce fMet-tRNA^{fMet}. The formyl group functions as a tag to interact with IF2 and to exclude the fMet-tRNA^{fMet} from the aa-tRNAs for elongation (Sundari *et al.* 1976). Formylation of Met-tRNA^{fMet} has been shown to be important for *E. coli* protein synthesis; where mutations in the anticodon sequence or the stem loop of the initiator tRNA reduce the Met-tRNA^{fMet} formylation, initiation activity is reduced *in vivo* (Varshney and RajBhandary 1992). There are three distinct features that can be found in fMet-tRNA^{fMet}, but not in elongator tRNA: (1) the absence of a Watson-Crick base pair between nucleotides 1:72 at the end of the acceptor stem, (2) the presence of three consecutive G·C base pairs at the bottom of the anticodon stem, and (3) the presence of a purine-11·pyrimidine-24 base pair in the dihydrouridine stem in contrast to a pyrimidine-11·purine-24 base pair in elongator tRNAs (Varshney *et al.* 1993). It has also been shown that the binding of IF2 to fMet-tRNA^{fMet} protects against the spontaneous hydrolysis of the aminoacyl ester bond in the tRNA, however, there is no protection of unformylated Met-tRNA^{fMet} (Petersen *et al.* 1979). X-ray crystal structures indicate that IF1 binds to the base of 30S subunit A-site in a cleft between the 530 loop and helix 44 of 16S rRNA and S12, and IF1 is thought to prevent the binding of initiator tRNA (Moazed *et al.* 1995; Carter *et al.* 2001).

The mRNA binds to the neck of the 30S subunit, with its 5'-untranslated region (UTR) containing the Shine-Dalgarno (SD) sequence which base pairs with the anti-SD sequence at the 3'-end of the 16S rRNA placing the initiation codon in the P-site allowing the binding of the initiator tRNA (Yusupova *et al.* 2001). It has been shown that IF2 forms specific interaction with fMet-tRNA^{fMet} to ensure the proper binding of fMet-

$tRNA^{fMet}$ with the start codon (Guenneugues *et al.* 2000). Subsequently, the pre-initiation complex consisting of the 30S ribosomal subunit, mRNA, initiator tRNA, IF1, IF2·GTP and IF3 then allows the release of initiator factors (IF1 and IF3), followed by the association of 50S subunit, and the hydrolysis of GTP bound to IF2. However, different studies reported controversial models with respect to the timing of the GTP hydrolysis by IF2. Tomsic *et al.* suggested that the proper positioning of fMet-$tRNA^{fMet}$ in the P-site and the release of IF2 from the ribosome does not require GTP hydrolysis (Tomsic *et al.* 2000). While Antoun *et al.* suggested that IF2·GTP promotes the association of the 50S subunit with the pre-initiation complex, and the GTP hydrolysis would trigger the release of IF2 from the ribosome (Antoun *et al.* 2003).

1.3 Elongation

After the initiation complex has formed, the P-site of the ribosome is occupied by fMet-$tRNA^{fMet}$ leaving the A-site empty and leading to the beginning of the elongation cycle. In each round of the cycle, one amino acid is added to the growing peptide chain, a process catalyzed by elongation factors Tu (EF-Tu), EF-Ts and EF-G (Figure 1.7). In brief, EF-Tu, GTP and aminoacyl-tRNA form a ternary complex that subsequently binds to the ribosome, catalyzing the codon-dependent binding of aa-tRNA to the ribosomal A-site. Upon codon-anticodon recognition, the conformation in the ribosomal decoding site changes, stabilizing aa-tRNA interaction and triggering GTP hydrolysis by EF-Tu. GTP hydrolysis causes structural changes in EF-Tu that subsequently result in the release of aa-tRNA into the ribosome. As EF-Tu dissociates from the ribosome, the CCA-end of the incoming tRNA enters the peptidyl transferase site on the 50S subunit, where the growing peptide waits for the newly incoming aa-tRNA. Following peptide bond formation

between the P- and A-site tRNAs, EF-G catalyzes the translocation of the P-site and A-site tRNAs along with mRNA into the E- and P-site, respectively; thus enabling the next round of the elongation cycle (Ramakrishnan 2002). Meanwhile, EF-Ts facilitates the nucleotide exchange in EF-Tu from the inactive GDP-bound to the active GTP-bound state of the protein. Therefore the elongation cycle can be divided into three phases: decoding, peptidyl transfer and translocation, which will be discussed in more detail in the following section.

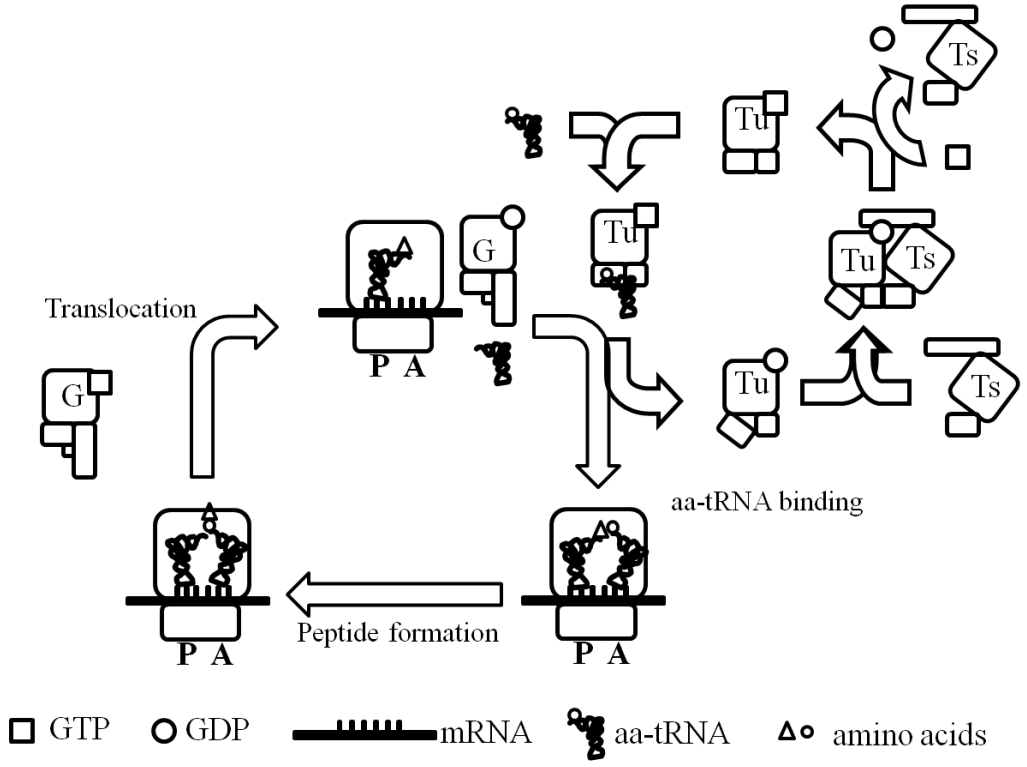

Figure 1.7 Elongation cycle in bacteria. The elongation cycle begins with the EF-Tu·GTP·aa-tRNA ternary complex delivering aa-tRNA to the ribosomal A-site. This is followed by peptide formation between the growing polypeptide in the P-site and incoming A-site amino acid on the aa-tRNA. Subsequently EF-G hydrolyses GTP to GDP facilitating the translocation of the concomitant P- and A-site tRNAs and the mRNA in the ribosome, resulting in an empty A-site exposing a new codon for the next round of elongation. EF-Ts facilitates the recycling of EF-Tu·GDP back to EF-Tu·GTP.

1.3.1 Decoding

The kinetics of EF-Tu-dependent aa-tRNA binding to the A-site has been studied by Pape *et al.* to a great detail (Pape *et al.* 1998). The error rate in translation is in the order of 10^{-3}-10^{-4} (Kurland 1992), hence, the codon recognition step is an important step during protein synthesis to ensure this high level of fidelity. However, there are two hypotheses to explain the mechanism of tRNA selection during decoding. The first hypothesis suggests that the decoding site on the 30S subunit recognizes codon-anticodon pairing sterically and screens for the cognate tRNA (Potapov 1982). The second model is known as the kinetic proofreading model, where the accuracy is based upon the rate differences of binding and dissociation favouring the binding of cognate over the non- or near-cognate tRNAs. According to this model, tRNA selection is separated into two steps: initial selection and proofreading; these steps are separated by EF-Tu catalyzed GTP hydrolysis (Hopfield 1974). Current studies suggest that the ribosome follows the second model (Pape *et al.* 1998).

During the decoding stage, aminoacyl-tRNA binds to EF-Tu·GTP forming a ternary complex that then binds to the ribosome. After the initial binding to the ribosome, codon-anticodon recognition takes place at the 30S ribosomal A-site, where the anticodon reversibly associates with the codon; the aminoacyl acceptor stem remains bound to EF-Tu. Pre-steady-state kinetic experiments suggest that the cognate tRNA not only has a lower dissociation rate than near-cognate tRNA, but also that it has faster rates of EF-Tu GTPase activation and aa-tRNA A-site accommodation (Pape *et al.* 1999). The X-ray crystal structure of ribosome in complex with tRNAs also revealed that correct codon recognition induces conformational changes of A1492 and A1493 in helix 44 as well as

the G530 of the 16S rRNA. The bases of the three nucleotides contact the minor groove of the codon-anticodon helix in the A-site, enabling the 16S rRNA to identify cognate tRNA by detecting correct Watson-Crick base pairing in the anticodon helix (Ogle *et al*. 2002).

The correct codon recognition induces the GTPase activation of EF-Tu was proposed in papers from Rodnina *et al.* and Piepenburg *et al.* (Rodnina *et al.* 1994; Piepenburg *et al.* 2000). However, the exact mechanism of the signal transmission from the decoding center at the 30S subunit to the G domain of EF-Tu at the 50S subunit is not clear. Studies using mutant variants of EF-Tu have shown that certain residues in EF-Tu may be involved in this signalling pathway (Jonak *et al.* 1982; Anborgh *et al.* 1992; Vorstenbosch *et al.* 1996). These variants will be discussed in more detail in Chapter 2. After the release of inorganic phosphate, EF-Tu changes from the GTP-bound to the GDP-bound conformation, which has a lower affinity to both the ribosome and the aa-tRNA, leading to the dissociation of EF-Tu from the tRNA and the ribosome (Yokosawa *et al.* 1975). Subsequently, the aa-tRNA in the ribosomal A-site can either undergo accommodation, where the aminoacyl end of the tRNA moves into the A-site of the 50S subunit, followed by peptide bond formation, or the aa-tRNA dissociates from the ribosome (Figure 1.8).

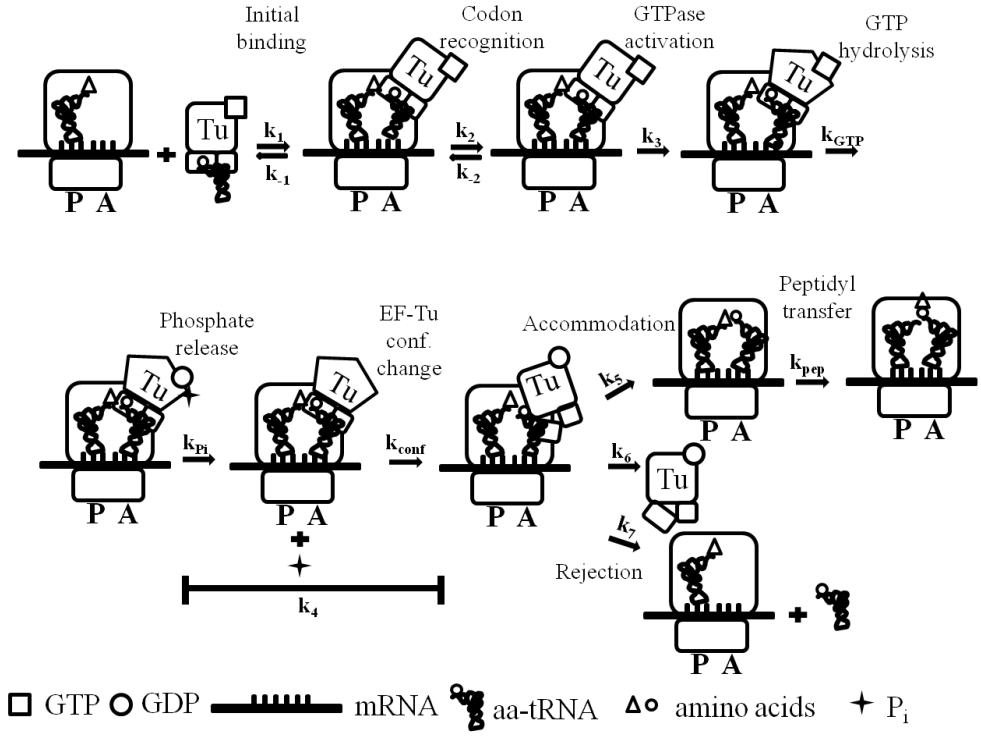

Figure 1.8 EF-Tu-dependent aa-tRNA binding to the ribosomal A-site. During initial binding, the EF-Tu·GTP·aa-tRNA ternary complex binds to the ribosome. After codon recognition, EF-Tu's GTPase activity is activated. Following the hydrolysis of GTP to GDP, inorganic phosphate is released, and EF-Tu changed its conformation to the EF-Tu·GDP bound form. Accommodation and peptidyl transfer occurred after correct codon recognition, and EF-Tu·GDP dissociates from the ribosome; or the near-cognate aa-tRNA is rejected from ribosomal A-site may occur.

In order to maintain fast *in vivo* protein synthesis, which is about 20 amino incorporated per second (Young and Bremer 1976), recycling of EF-Tu back into the GTP-bound form is required in order to not deplete the cellular pool of EF-Tu·GTP. EF-Tu has a 100-fold higher affinity for GDP than GTP, and GDP dissociation is very slow (Gromadski *et al.* 2002). Therefore, nucleotide exchange is limited by the rate of nucleotide dissociation and the cellular concentration difference between the two nucleotides. Hence, EF-Ts, the guanine nucleotide exchange factor for EF-Tu, is required

to facilitate the efficient exchange of GDP for GTP in EF-Tu. The interaction between EF-Tu and EF-Ts will be discussed in more details in Chapter 2.

1.3.2 Peptidyl Transfer

After accommodation, the aminoacyl end of the tRNA enters the peptidyl transferase center (PTC) on the 50S subunit, which is followed by rapid peptide bond formation (Pape *et al.* 1998). During peptide bond formation, the α-amino group from the incoming A-site tRNA performs a nucleophilic attack on the carbonyl carbon of the P-site tRNA resulting in a peptide bond between the peptidyl residue and the aminoacyl group at the A-site (Satterthwait and Jencks 1974) (Figure 1.9)

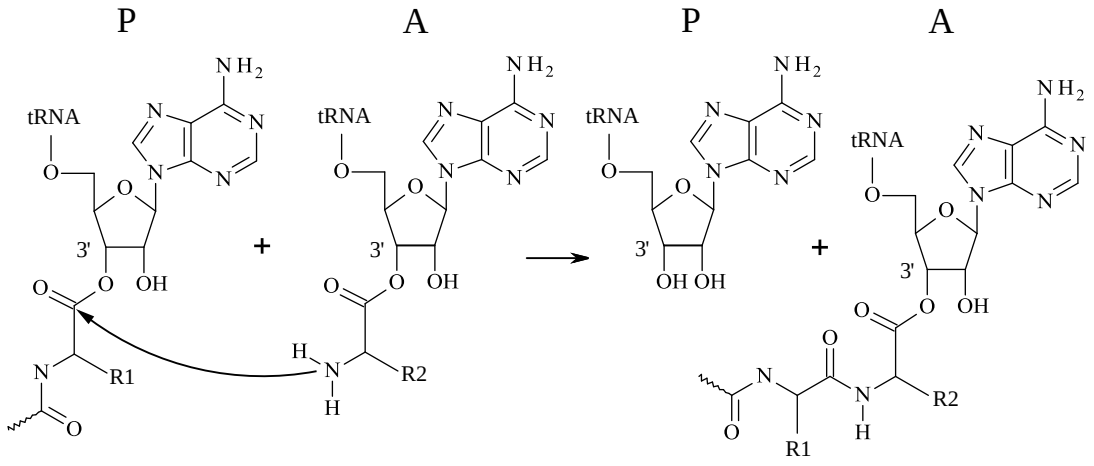

Figure 1.9 Peptide-bond formation on the ribosome. Both aminoacyl groups of the P- (left) and A-site (right) tRNA are attached to the ribose at the 3' position via an ester bond; nucleophilic attack from the A-site tRNA on the P-site tRNA results in peptide bond formation (Pech and Nierhaus 2008).

1.3.3 Translocation

After peptide bond formation, the P-site is occupied by a deacylated tRNA and the A-site containes the newly formed peptidyl-tRNA. In order to enable the next round

of the elongation cycle, the P- and A-site tRNA need to be moved into the E- and P-site, respectively. This translocation step is catalyzed by elongation factor G (EF-G). Previous studies have revealed that a slow rate of translocation can be observed even in the absence of EF-G, suggesting that translocation of tRNAs may be due to the movement of the ribosome, and thus EF-G acts as a factor to lower the kinetic energy barrier through binding to the ribosome (Gavrilova and Spirin 1971). Rapid kinetics studies confirmed that EF-G facilitates tRNA movement during translocation (Inoue-Yokosawa *et al.* 1974; Rodnina *et al.* 1997). After the binding of EF-G·GTP to the ribosome, GTP hydrolysis takes place. The release of inorganic phosphate leads to a conformational change in EF-G and subsequent changes in the ribosome, causing the movement of the tRNA·mRNA complex. After the dissociation of EF-G·GDP and the deacylated-tRNA, the ribosome bound to mRNA and tRNAs form the respective post-translocation complex that is ready for a new incoming aa-tRNA (Katunin *et al.* 2002)

1.4 Termination and ribosome recycling

The termination of protein synthesis takes place when a stop codon is read in the ribosomal A-site by one of the release factors (RF). In bacteria, the release factors can be subdivided into two classes. Although both class I proteins (RF1 and RF2) recognise the UAA codon, RF1 also responds to UAG, while RF2 responds to UGA (Kisselev and Buckingham 2000). Termination begins with the binding of RF1 or RF2 to the respective stop codon on the mRNA in the ribosomal A-site, this triggers the hydrolysis of the aminoacyl ester bond that links the nascent growing polypeptide to tRNA in the ribosomal P-site (Nakamura and Ito 2003). After the release of the polypeptide chain, the class II release factor (RF3) binds as a binary complex with GTP to the ribosome and

induces the release of RF1 or RF2 (Freistroffer *et al.* 1997). However, the exact mechanism for RF involvement in translation termination remains unclear.

After termination, the ribosome remains bound to the mRNA and deacyl-tRNA in the P-site. In order to facilitate the reinitiation of the ribosome, the complex has to be disassembled and the mRNA and the tRNA have to be released. Ribosome recycling factor (RRF) and EF-G are required for this process (Janosi *et al.* 1996). Interestingly, the details of how RRF interacts with EF-G and disassembles the post-termination ribosome complex is not known. It has been proposed that before the release of RRF from the ribosome, RRF moves from the A/P site to the P/E site clashing with the tRNA (Agrawal *et al.* 2004). In the presence of the EF-G specific inhibitor thiostrepton or translocation-impaired mutant EF-Gs, disassembly of the complex fails, suggesting that EF-G facilitated release of RRF is required for post-termination complex disassembly (Kiel *et al.* 2003). However, it has also been suggested that the RRF disassembles the ribosomal complex independently of the translocation activity of EF-G (Fujiwara *et al.* 2004), and IF3 promotes the dissociation of tRNA from the P-site (Karimi *et al.* 1999). This model is in agreement with the kinetic studies of ribosome recycling (Peske *et al.* 2005). Therefore, it is still unclear what the function of EF-G during ribosomal recycling is.

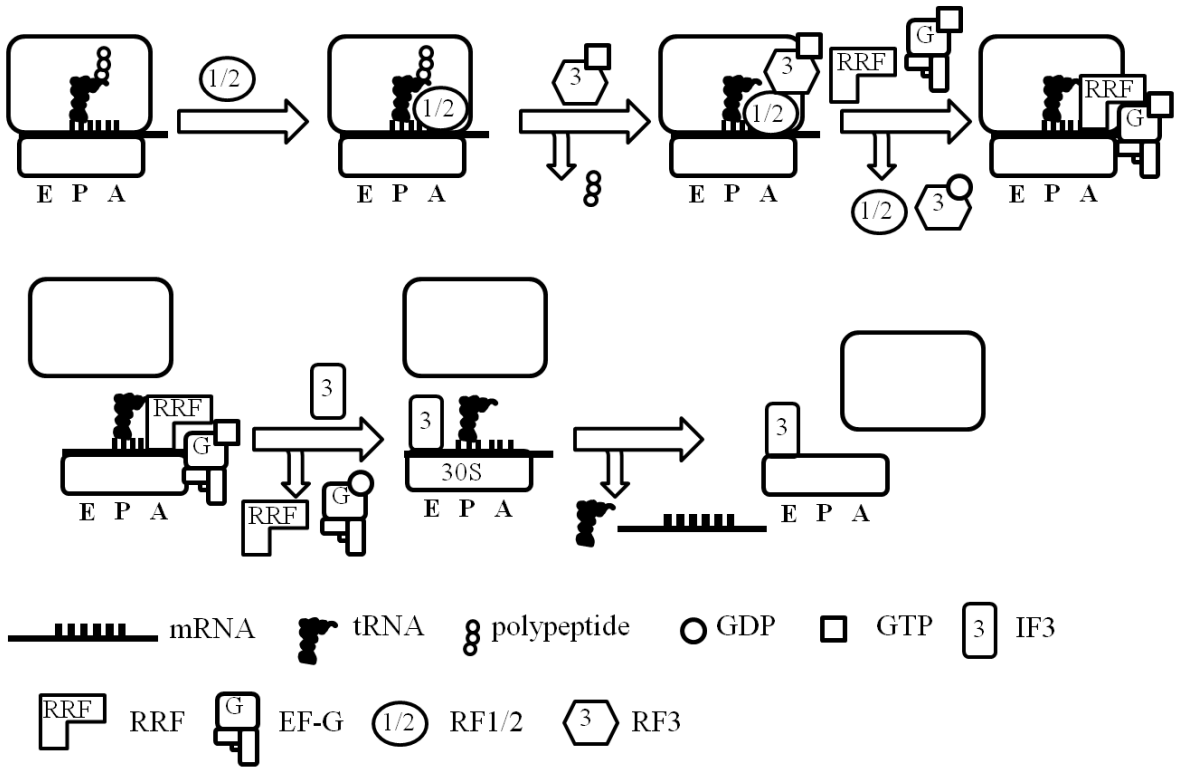

Figure 1.10 Termination and ribosome recycling. The ribosome on the top left has a stop codon in the A-site. RF1 or RF2 bind to the ribosome and induce the release of the polypeptide chain. After the binding of RF3·GTP to the complex, GTP is hydrolyzed, causing the dissociation of RF1, RF2 and RF3. This allows the binding of RRF and EF-G, subsequent GTP hydrolysis by EF-G catalyzes the dissociation of the two ribosomal subunits. After the dissociation of RRF and EF-G from the ribosomal subunit, IF3 binding facilitates the release of mRNA and tRNA from the 30S subunit, allowing reprogramming and initiation complex formation.

Chapter 2 EF-Tu

2.1 EF-Tu

EF-Tu is probably the best studied protein involved in protein synthesis. It is also a functional and structural model for the study of translational GTPases. EF-Tu belongs to the regulatory GTPase superfamily, which function as molecular switches regulating a large number of cellular processes. The common features of this family can be summarised as (1) the cycling between an active and an inactive conformation depending on whether GTP ("on" state) or GDP ("off" state) is bound; (2) a very low intrinsic GTPase and GDP/GTP exchange activity. The low intrinsic GTPase activity is dramatically enhanced by the interaction of the G protein with its GTPase activating protein (GAP). The rate of nucleotide exchange for the G protein can be increased through the interaction with a guanine nucleotide exchange factor (GEF), as well as inhibited by the respective guanine nucleotide dissociation inhibitors (GDIs). For EF-Tu, the GAP and GEF are the ribosome and EF-Ts, respectively (Krab and Parmeggiani 2002). However, no GDI has been identified for EF-Tu so far. During protein synthesis, EF-Tu in its active form is bound to GTP and facilitates aa-tRNA binding to the A-site of the translating ribosome. After the cognate anticodon of the tRNA interacts with the respective mRNA codon, EF-Tu hydrolyses GTP and changes its conformation to the inactive GDP bound form. EF-Tu then releases the bound aa-tRNA onto the ribosome and dissociates from the ribosome while remaining bound to GDP. Subsequently, EF-Ts facilitates the change of EF-Tu from the GDP-bound form to the GTP-bound form enabling EF-Tu to bind to another aa-tRNA and to enter another round of the elongation cycle.

Escherichia coli EF-Tu contains 394 amino acids, and is divided into three domains. Domain I of EF-Tu, also known as the G domain, contains the guanine nucleotide binding site. The binding of nucleotide to EF-Tu involves several conserved sequence motifs, the so-called G motifs, which are shared by all G proteins. The G1 motif $Gx_4GK(S/T)$ is involved in the binding of the guanine nucleoside triphosphates, the G2 DxxG is involved in the conformational changes taking place during the transitions from the GDP to the GTP form of EF-Tu, and the G3 NKxD determines the specificity for guanine (Kjeldgaard *et al.* 1996). The GDP- and GTP-bound form of EF-Tu have different conformations, and two segments of the polypeptide chain, switch I and II, act as sensors for the presence or absence of the γ-phosphate. Structural studies have shown that the switch I region, residues 53-59, undergoes a conformational change from a β-sheet structure in the GDP form, to an α-helical structure in the GTP form (Abel *et al.* 1996). While, the switch II region, residues 83-99, unwinds one helical turn at its N-terminus and forms another one at the C-terminal end, helix B, residues 84-92, is tilted by 42^o (Song *et al.* 1999). The movement of switch II region from the GTP to the GDP form was suggested to be due to the removal of the extra negative charge of the γ-phosphate group. During the transition from the GDP-bound to the GTP-bound state, domain I rotates about 90^o relative to domain II and domain III, causing EF-Tu to form a closed conformation rather than the open form in the GDP bound state (Song *et al.* 1999). Hence, domain I is much closer to domain III in the GTP bound form. However, the interaction between domain II and domain III is very similar in the GDP and GTP-bound form (Figure 2.1). A magnesium ion is an essential factor for GTP binding and GTPase activation in G proteins (Gilman 1987). When EF-Tu binds to a guanine nucleotide, the

Mg^{2+} is important for the proper positioning of the nucleotide in the binding pocket through hydrogen bonding interaction (Song *et al.* 1999). The role of Mg^{2+} for nucleotide binding can be demonstrated by treatment with EDTA, chelating Mg^{2+} from EF-Tu, which results in a dramatic decrease in nucleotide affinity (Krab and Parmeggiani 2002).

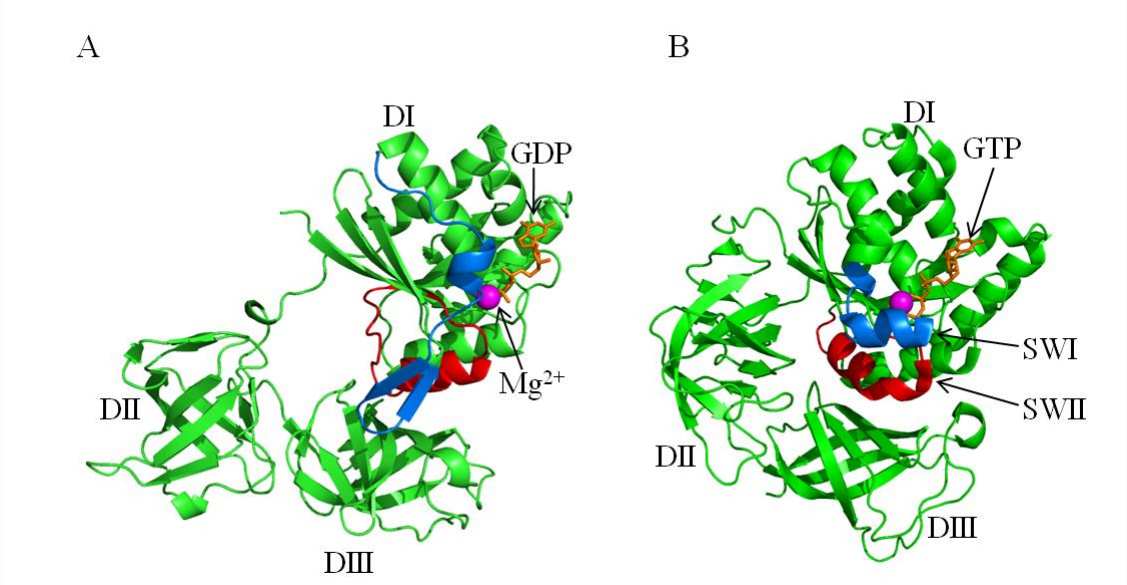

Figure 2.1 Structure comparison of EF-Tu in two conformations. Cartoon diagram of *Escherichia coli* EF-Tu·GDP (A) (PDB: 1EFC) and *Thermus thermophilus* EF-Tu·GTP (B) (PDB: 1EXM). EF-Tu is shown in green, Mg^{2+} in magenta, GDP/GTP in orange, switch I (SWI) region and switch II (SWII) region of EF-Tu in blue and red, respectively.

The EF-Tu·GTP binary complex has been shown to have a high affinity for aa-tRNA (Pingoud *et al.* 1977). Formation of the binary complex allows binding of aa-tRNA resulting in an EF-Tu·GTP·aa-tRNA ternary complex (Figure 2.2). *Escherichia coli* contains 41 different tRNA species with different anticodons (Laursen *et al.* 2005). Although EF-Tu cannot discriminate between correctly and incorrectly amino-acylated tRNAs, it efficiently discriminates between the aa-tRNA and deacylated tRNA (Pingoud

et al. 1977). Nissen *et al.* reported the crystal structure of the ternary complex in 1995, allowing for the first time the detailed visualization of the interaction between EF-Tu and an aa-tRNA (Phe-tRNA^{Phe}) at atomic level (Nissen *et al.* 1995). The structure revealed that all three domains of EF-Tu are involved in aa-tRNA binding, and interactions take place at the 3'-CCA-end, the 5'-end and the T stem of the aa-tRNA (Nissen *et al.* 1995). The affinity for deacylated tRNA binding to the binary complex has been shown to be 4 to 5 orders of magnitude lower than the one of aa-tRNA binding (Shulman *et al.* 1974). Nissen and co-workers further suggested that the recognition of aa-tRNA by EF-Tu involves the aminoacyl ester bond and the backbone conformation of the acceptor helix (Nissen *et al.* 1996). The 3'-CCA-Phe binds to a cleft between domain I and domain II, and interacts with domain II residues through hydrogen bonding (Nissen *et al.* 1996).

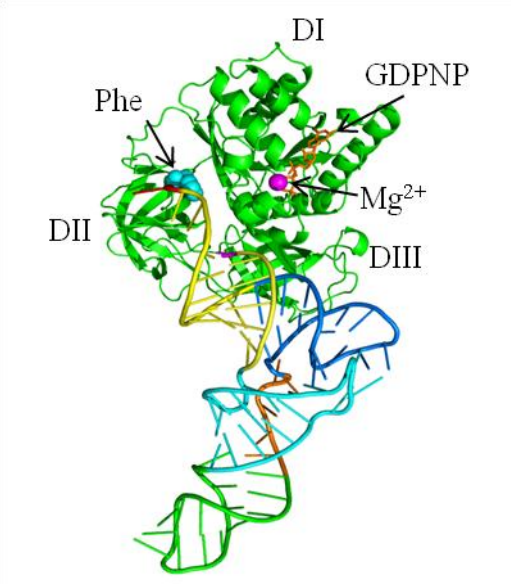

Figure 2.2 X-ray structure of the ternary complex of yeast Phe-tRNA^{Phe}, *Thermus aquaticus* EF-Tu and GDPNP (PDB: 1TTT). EF-Tu domain I, II and III are shown in green, Mg^{2+} in magenta, GDPNP in orange. The Phe-tRNA^{Phe} 3'-end is coloured in red, acceptor stem in yellow, TψC loop in blue, variable loop in orange, the anticodon loop in green, the D loop in cyan, 5'-end in magenta and the amino acid Phe is in cyan.

Formation of the ternary complex facilitates the delivery of aa-tRNA to the programmed ribosome. Upon binding to the ribosome, aa-tRNA enters the A-site of the 30S subunit and remains bound to EF-Tu. When the codon-anticodon interaction triggers EF-Tu's GTPase activity, rapid GTP hydrolysis results in a conformational change in EF-Tu. The subsequent release of aa-tRNA into the ribosome is followed by the dissociation of EF-Tu from the ribosome (Pape *et al*. 1998). Cryo-EM structures have shown that the ternary complex binds to both the 30S and the 50S subunit A-site (Stark *et al.* 2002). On the 30S subunit, the anticodon stem-loop (ASL) of the tRNA occupies the decoding center, the minor groove of the D stem contacts ribosomal protein S12, and the T loop of the aa-tRNA forms interaction with the 23S rRNA in the 50S subunit (Stark *et al.* 2002). EF-Tu domain I interacts with the sarcin-ricin stem-loop (SRL) of the 23S rRNA and the L12 ribosomal protein on the 50S subunit (Stark *et al*. 2002; Villa *et al*. 2009); and domain II of EF-Tu contacts the 16S rRNA (Schuette *et al.* 2009). Val 20 and Ile 60 in EF-Tu have been proposed to form a hydrophobic gate that only opens in the presence of the ribosome, and that allows the side chain of the catalytic residue His 84 to reach the GTP binding pocket and to activate GTP hydrolysis (Dahl *et al.* 2006; Villa *et al.* 2009). Molecular modeling has suggested that the ribosome-stimulated GTP hydrolysis by EF-Tu is promoted by the conformational rearrangement of the His 84 side chain approaching to the active site (Grigorenko *et al.* 2008). Based on the cryo-EM structure, Villa *et al.* proposed that L12 induced the conformational rearrangements of EF-Tu and reorientation of the catalytic His 84 which then leads to GTP hydrolysis (Villa *et al.* 2009). It has also been proposed that local flexibility in the tRNA and mRNA might also allow signal transmission, and that the interactions of the ribosome with the ternary

complex will stabilize the conformation of EF-Tu in the state required for GTP hydrolysis (Schuette *et al.* 2009). However, the details of signal transmission from the decoding center to trigger GTPase activation on EF-Tu remain unclear.

After EF-Tu·GDP has dissociated from the ribosome and in order for it to participate in the next round of the elongation cycle, EF-Tu must return to the active form by exchanging the bound GDP for GTP (Figure 2.3). However, the dissociation of GDP from EF-Tu is very slow (0.002 s^{-1}) and requires the action of EF-Tu's GEF EF-Ts. EF-Ts binds to EF-Tu and causes a thousand-fold decrease in the affinity of EF-Tu for GDP (Gromadski *et al.* 2002). The structure of the *E. coli* EF-Tu·EF-Ts complex revealed that domain I of EF-Tu interacts with the subdomain N, the N-terminal domain, and the C-terminal domain of the EF-Ts, whereas EF-Tu domain III contacts the EF-Ts subdomain C (Figure 2.4) (Kawashima *et al.* 1996). More importantly, the binding of EF-Ts to EF-Tu causes a conformational change in the P loop of EF-Tu's G domain, which leads to changes in the nucleotide binding affinity. It also disrupts the Mg^{2+}-coordination and may change the orientation of the ribose binding sites (Wieden *et al.* 2002).

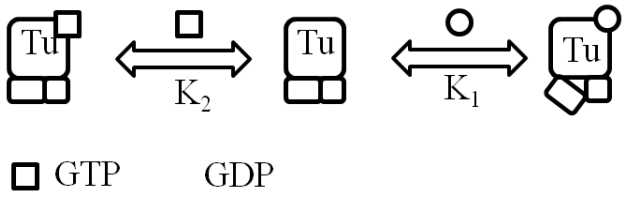

Figure 2.3 Kinetic scheme of nucleotide exchange in EF-Tu.

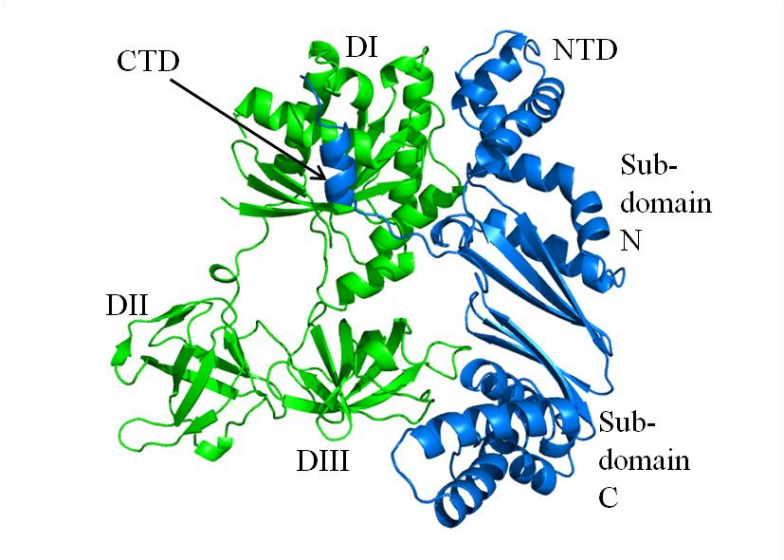

Figure 2.4 Interactions between *E. coli* EF-Tu and EF-Ts (PDB: 1EFU). EF-Tu is shown in green, containing three domains: DI, DII and DIII. EF-Ts is shown in blue and consists of four domains: N-terminal domain (NTD), subdomain N, subdomain C and C-terminal domain (CTD).

Although Pape *et al.* reported a rate for the GTP-GDP conformational change of EF-Tu during ribosomal A-site binding (Pape *et al.* 1998), it is unclear how EF-Tu changes its conformation during this process. Elongation factor Tu adopts two different conformations dependent on the guanine nucleotide bound, a closed conformation when bound to GTP and an open conformation when bound to GDP. One of the methods to study the domain movement within EF-Tu, to enable further understanding of the protein's dynamic communication networks, is through fluorescently labelling EF-Tu. In the open conformation, the distance between domain I and domain II of EF-Tu is much larger than in the closed conformation. Therefore, by labelling residues in domain I and II with fluorescent dyes will allow a detailed study of domain movement within EF-Tu during its interaction with either aa-tRNA or the ribosome.

EF-Tu forms a ternary complex with GTP and aa-tRNA and binds to the ribosomal A-site. The ternary complex bound to the ribosome has been studied by cryo-EM and X-ray techniques (Stark *et al.* 2002; Schuette *et al.* 2009; Villa *et al.* 2009). These studies have identified specific interactions between the different factors that are involved in translation. Kinetic studies have revealed the rate constants for each individual step (Pape *et al.* 1998; Gromadski *et al.* 2002; Katunin *et al.* 2002). However, the signal transmissions and dynamic communication network behind them remain unclear. For example, crystal structures have shown the binding site of the nucleotide on the EF-Tu (Kjeldgaard *et al.* 1993; Song *et al.* 1999) and kinetic studies have demonstrated that the ribosome stimulates EF-Tu's GTPase activity only after codon recognition (Pape *et al.* 1998). But only little is known about how codon-recognition triggers GTPase activation in EF-Tu, and how the aa-tRNA is released from EF-Tu, enabling it to swing into the PTC which requires a 70 Å movement (Rodnina *et al.* 2005). It has been shown that the ribosome-stimulated GTP hydrolysis of EF-Tu with the presence of aa-tRNA is much faster than the one without the aa-tRNA (Thompson *et al.* 1986). Moreover, Piepenburg *et al*. showed that in the presence of interrupted tRNAs, EF-Tu cannot hydrolyze GTP as fast as the one with continued aa-tRNA; suggested that tRNA is required for GTPase activation signal transmission from the decoding site to EF-Tu (Piepenburg *et al.* 2000). More interestingly, aa-tRNAs have different nucleotide sequences, but it is unclear how this universal GTPase activation signal can be transmitted through different tRNA to EF-Tu in such efficient way.

It is therefore necessary to study the dynamic communication networks between each factor involved in protein synthesis and, more importantly, the functional role of the

conserved amino acid residues in EF-Tu, which may be also required for the development of new tools in order to understand the details of this process.

2.2 Objective

In this thesis, two questions will be addresssed:

- Can the highly conserved residue Cys 81 in EF-Tu be replaced by Ala, Met or Ser without altering the affinity of EF-Tu for guanine nucleotides, the aa-tRNA and the ribosome, to enable the Cysteine specific introduction of fluorescent on a non-fluorescen reporter group?
- Are residues R279, G280 and R283 in EF-Tu involve in the GTPase activation pathway of EF-Tu?

Chapter 3 Material and Methods

3.1 Protein overexpression and purification

3.1.1 Overexpression

For the overexpression of 6x-Histidine-tagged EF-Tu, pEECAHIS plasmids coding for wild-type *tuf*A gene and the respective mutant EF-Tus were transformed into *Escherichia coli* BL21-DE3 cells (Novagen), plated on Luria Broth (LB) ampicillin agar plates, and incubated over night at 37^{o}C. A single colony was picked and used to inoculate an overnight culture of 50 mL LB medium with 100 μg/mL ampicillin at 37^{o}C.

Overnight cultures were centrifugated at 5,000 xg for 10 min at 4^{o}C (Legend®, Sorvall), and washed with 5 mL LB. The resuspended cell pellet was used to inoculate fresh LB medium supplemented with 100 μg/mL ampicillin to an optical density $(OD)_{600}$ of about ~ 0.1. Cultures were grown at 37^{o}C to an OD_{600} of 0.6, and protein overexpression was induced by addition of isopropyl β-D-1 thiogalactopyranoside (IPTG) to a final concentration of 1 mM. After induction, cells were grown for 3 hrs and harvested by centrifugation at 5,000 xg for 10 min in a TA-10 rotor (Beckman), flash frozen and stored at -80^{o}C for future use. To confirm the overexpression of EF-Tu, 1 OD_{600} of cells was taken every hour, lysed in 8 M urea solution in water and then analyzed on a 12% SDS-PAGE at 200V for 1 hr (bio-Rad Mini-PROTEAN Tetra Cell) and stained by Coomassie blue.

3.1.2 Purification of recombinant EF-Tu

Cells containing either wild-type or EF-Tu variants (10 g) were resuspended in 7 mL of Buffer A per gram of cells (50 mM Tris-Cl pH 8.0 at 4^{o}C, 60 mM NH_4Cl, 7 mM $MgCl_2$, 7 mM β–mercaptoethanol, 1 mM phenylmethylsulfonylfluoride (PMSF), 50 μM

GDP, 300 mM KCl, 10 mM imidazole and 15% v/v glycerol), then opened by incubation on ice for 30 min with lysozyme at a final concentration of 1 mg/mL. After the addition of 12.5 mg/g of sodium deoxycholate, the viscosity of the solution increased. The solution was then sonicated until the viscosity decreased again. The cell debris was removed by centrifugation at 3,000 xg for 30 min at 4°C (Legend®, Sorvall). To harvest the S-30 extract, the resulting supernatant was centrifuged for 45 min at 30,000 xg at 4°C in a JA-16 rotor (Beckman).

The S-30 extract was applied to a 5 mL Ni^{2+}-Sepharose column (GE Healthcare) and incubated on ice for 45 min, the supernatant was then removed by centrifugation at 500 xg for 5 min at 4°C (Legend®, Sorvall). To remove unspecifically bound proteins, the resin was washed 3 times with 40 mL of Buffer A, and 4 times with Buffer B (50 mM Tris-Cl pH 8.0 at 4°C, 60 mM NH_4Cl, 7 mM $MgCl_2$, 7 mM β-mercaptoethanol, 1 mM PMSF, 50 μM GDP, 300 mM KCl, 20 mM imidazole and 15% v/v glycerol). His-tagged EF-Tu was eluted by incubating the resin 10 times with 9 mL of Buffer C (50 mM Tris-Cl pH 8.0 at 4°C, 60 mM NH_4Cl, 7 mM $MgCl_2$, 7 mM β-mercaptoethanol, 1 mM PMSF, 50 μM GDP, 300 mM KCl, 250 mM imidazole and 15% v/v glycerol). 100 μl samples were collected during each wash step, and analyzed by 12% SDS-PAGE at 200 V for 1 hr and subsequently stained with Coomassie blue. Elution fractions containing EF-Tu were pooled and concentrated with Vivaspin 20 (30,000 MWCO, Sartorius stedim) to a final concentration of ~ 100 μM.

The proteins were further purified and re-buffered by size exclusion chromatography (SEC) using a Superdex 75 column (XK26/100, GE Healthcare) in

$TAKM_7$ (50 mM Tris-Cl pH 7.5 at 4 ^oC, 70 mM NH_4Cl, 30 mM KCl and 7 mM $MgCl_2$). Fractions were analyzed on a 12% SDS-PAGE at 200 V for 1 hr and stained by Coomassie blue. Fractions containing EF-Tu were pooled, concentrated to ~ 100 μM, shock frozen in liquid nitrogen, and stored at -80 ^oC.

The purity of the protein was analyzed by loading 100 pmol of each protein on a 12% SDS-PAGE at 200V for 1hr, and stained by Coomassie blue. All purified EF-Tu proteins were at least 90% pure.

3.2 Rapid kinetic measurements

Fluorescence stopped-flow measurements were performed with a KinTek SF-2004 stopped-flow apparatus as described previously (Wieden *et al.* 2010). In brief, fluorescence resonance energy transfer (FRET) from the single residue Trp184 in EF-Tu to the 2'-(or -3')-*O*-(*N*-methylanthraniloul) (mant)- group of the fluorescently-labelled nucleotide analog (mant-GDP or mant-GTP) (Invitrogen) was measured. This was carried out by exciting Trp184 at 280 nm and detecting the resulting mant-fluorescence after passing LG-400-F cut-off filter (NewPort).

Guanine nucleotide dissociation rate constants (k_{-1}, k_{-2}) were measured by rapidly mixing equal volumes (25 μl) of 0.6 μM EF-Tu·mant-GDP/mant-GTP with 30 μM GDP/GTP in $TAKM_7$ at 20 ^oC, and monitoring the time courses of mant fluorescence. Under these conditions, the large excess of unlabelled nucleotide limits the rebinding of mant-GDP/mant-GTP to EF-Tu, and the fluorescence change only reflects the dissociation of the mant-nucleotide. The data were evaluated by fitting the time courses

to a single-exponential function: F= A+B*exp(-*kt*), where F is the fluorescence at time *t*, A is the final fluorescence, B is the amplitude and the *k* is the dissociation rate constant.

EF-Ts stimulated mant-GDP/mant-GTP dissociation rates (k_{appTs}) were measured by rapidly mixing equal volumes (25 μl) of 0.6 μM EF-Tu·mant-GDP/mant-GTP and 30 μM GDP/GTP, 2 μM EF-Ts in $TAKM_7$ at 20 ^oC, and monitoring the time course of fluorescence change of the mant emission.

The apparent rate constant of nucleotide association to EF-Tu was measured by rapidly mixing equal volumes (25 μl) of 0.6 μM nucleotide free EF-Tu with different concentrations of mant-GDP/mant-GTP (0.6 to 10 μM) in $TAKM_7$ at 20 ^oC, and monitoring the time courses of mant-fluorescence change. Data were evaluated by fitting the time courses with an one exponential association function: F=A+B*exp(-$k_{app}t$), where k_{app} is the apparent rate constant of association, F is the fluorescence at time *t*, A is the final fluorescence and B is the amplitude. The obtained apparent rate constants were plotted against increasing concentrations of nucleotide, and subsequently fitted with a linear equation. The slope of the linear equation thus gives the respective association rate constant (k_1, k_2).

Data fitting was performed using the TableCurve software (Jandel Scientific), and normalized using the GraphPad Prism software by setting the highest point in the curve as 100% and the lowest point as 0% (GraphPad Software, Inc.).

3.2.1 Purification of nucleotide-free EF-Tu

To purify EF-Tu from bound GDP, 10,000 pmol EF-Tu·GDP were incubated in TAE buffer (50 mM Tris-Cl pH 7.5 at 4°C, 70 mM NH_4Cl, 10 mM EDTA) in a final volume of 250 µl for 30 min at 37 °C to remove the Mg^{2+} from the complex releasing the bound nucleotide. GDP and EF-Tu were separated by SEC on an Acorn Superdex 75 10/300 GL column (GE healthcare) with TA buffer (50 mM Tris-Cl pH 7.5 at 4°C, 70 mM NH_4Cl). The protein containing fractions were detected by OD_{280} readings on a UV spectrometer, and those containing at least 0.6 µM EF-Tu were pooled and stored on ice. Nucleotide free EF-Tu was stable within the time of the experiment and retained the characteristics of untreated EF-Tu with respect to the binding of GDP/GTP (Wieden *et al.* 2010).

3.2.2 Preparation of EF-Tu·mant-GDP and EF-Tu·mant-GTP

To form EF-Tu·mant-nucleotide binary complex, 0.6 µM EF-Tu was incubated with 6 µM mant-GDP or mant-GTP (Invitrogen) for 30 min at 37 °C in $TAKM_7$. When EF-Tu was incubated with mant-GTP, 3 mM phosphoenolpyruvate (PEP) and 0.1 mg/mL pyruvate kinase (PK) (Roche) were also added to the reaction to convert GDP or mant-GDP to GTP or mant-GTP, respectively.

All purified EF-Tu variants were at least 80% active compared to wild-type protein.

3.3 Purification of ribosomes

Frozen *E. coli* MRE 600 cells (50 g) were crushed and ground with 100 g of cold Al_2O_3 in a cold mortar for 30 min at 4°C. DNase I was added to the mixture and mixed for 10 min, followed by the addition of opening buffer (20 mM Tris-HCl pH 7.6, 100 mM NH_4Cl, 10.5 mM $MgCl_2$, 0.5 mM EDTA, 3 mM β-mercaptoethanol) to 120 mL. The mixture was then centrifuged at 1,000 xg for 10 min, then 10,000 xg for 30 min with a Beckman JA-14 rotor. The supernatant was further centrifuged at 30,000 xg for 30 min in a Beckman Ti-45 rotor. 40 mL of the resulting supernatant was overlaid onto a 20 mL sucrose cushion (20 mM Tris-HCl pH 7.6, 500 mM NH_4Cl, 10.5 mM $MgCl_2$, 0.5 mM EDTA, 1.1 M Sucrose, 3 mM β-mercaptoethanol) and centrifuged at 200,000 xg for 16 hrs in a Beckman Ti-45 rotor. Pellets were dissolved in washing buffer (20 mM Tris-HCl pH 7.6, 500 mM NH_4Cl, 10.5 mM $MgCl_2$, 0.5 mM EDTA, 7 mM β-mercaptoethanol) and pooled; the volume was then adjusted to 100 mL with washing buffer. 50 mL of the solution was subsequently overlaid onto a 4 mL sucrose cushion and centrifuged at 200,000 xg for 14.5 hrs in a Beckman Ti-45. The resulting pellets were dissolved in 20 mL washing buffer, and the volume was adjusted to 60 mL. 10mL of the solution were overlaid onto a 1.5 mL sucrose cushion and centrifuged at 141,000 xg for 13 hrs in a Beckman SW28. Pellets were then dissolved in 40 mL overlay buffer (20 mM Tris-HCl pH 7.6, 60 mM NH_4Cl, 5.25 mM $Mg(OAc)_2$, 0.25 mM EDTA, 2 mM β–mercaptoethanol) with 5mL 50% sucrose buffer (20 mM Tris-HCl pH 7.6, 60 mM NH_4Cl, 5.25 mM $Mg(OAc)_2$, 0.25 mM EDTA, 50% sucrose, 3 mM β–mercaptoethanol). The concentration of this pre-zonal solution was determined by A_{260} measurement using an extinction coefficient of 23 pmol/OD_{260}.

70S ribosomes and ribosomal subunits were separated by zonal centrifugation. 400 mL of overlay buffer was loaded into a Beckman Ti-15 zonal rotor at 200 xg at 4°C, then 22.5 mL (10,000 – 15,000 OD_{260} units) of pre-zonal ribosome solution was loaded into the rotor, followed by the addition of a 1370 mL 10% - 40% sucrose gradient (20 mM Tris-HCl pH7.6, 60 mM NH_4Cl, 5.25 mM $Mg(OAc)_2$, 0.25 mM EDTA, 3 mM β-mercaptoethanol, and 10% to 40% sucrose) until 150 mL of overlay buffer came out of the outlet tube. Lastly, 150 mL of 50% sucrose buffer was loaded into the rotor and centrifuged at 42,000 xg for 19 hrs at 4°C. Fractions were measured at OD_{260} and those containing 70S, 50S and 30S were pooled and centrifuged at 200,000 xg for 46 hrs in a Beckman Ti-45 at 4°C. The resulting pellets were then dissolved in the final storage buffer (20 mM Tris-HCl pH7.6, 50 mM NH_4Cl, 5 mM $MgCl_2$) and the concentration adjusted to around 10 μM. Ribosomes were aliquoted and flash frozen in liquid nitrogen and stored at -80°C.

3.4 Purification of [^{14}C] Phe-tRNA^{Phe}

To aminoacylate tRNA^{Phe}, 10 μM *E. coli* tRNA^{Phe} (Sigma), 40 μM [^{14}C] Phe (MP-Biomedical), 5% crude synthetase, 3 mM ATP (Sigma) were incubated in aminoacylation buffer (25 mM Tris-OAc pH 7.5, 8 mM $Mg(OAc)_2$, 100 mM NH_4OAc, 30 mM KOAc, 1mM DTT) to a final volume of 500 μL. [^{14}C] Phe-tRNA^{Phe} was separated from tRNA^{Phe} using a linear ethanol gradient from Buffer D (20 mM NH_4OAc pH 5, 10 mM $Mg(OAc)_2$, 400 mM NaCl) to Buffer E (20 mM NH_4OAc pH 5, 10 mM $Mg(OAc)_2$, 400 mM NaCl, 30% ethanol) on a Jupiter 5μ C_{18} 300A reverse phase

chromatography column (Phenomenex) on an HPLC (BioCad Sprint Perfusion Chromatography system).

3.5 Dipeptide formation

10 μl of solution I containing 0.5 μM 70S ribosomes and 1mg/mL poly(U), and 10 μl of solution II containing 1 μM EF-Tu, 1 mM GTP, 3 mM PEP and 0.2 mg/mL PK were individually incubated in Buffer F (50 mM Tris-HCl pH 7.5, 70 mM NH_4Cl, 30 mM KCl, 10 mM $MgCl_2$ and 1 mM DTT) at 37°C for 15 min. Both solution I and II were mixed with 5 μl of 1 μM [^{14}C] Phe-tRNA^{Phe} and incubated at 37°C for 30 s. The two solutions were then mixed and incubated for additional 30 s. The reaction was quenched with 30 μl of 2 M KOH and further incubated at 37°C for 15 min. Finally 60 μl of glacial acetic acid was added and the solution was centrifuged at 11,500 xg for 10 min using a Hermel Z180M (Labnet International, Inc) centrifuge. 60 μl of the supernatant were removed and added to 125 μl of Buffer G (0.1% TFA in H_2O). Dipeptides formed were separated from the supernatant using a 0-100% linear gradient from Buffer G to Buffer H (0.1% TFA, 65% Acetonitrile) on a EC 250/4 NUCLEOSIL 100-5 C_{18} column (Macherey-Nagel) on a Breeze HPLC (Waters). Fractions were analyzed in a Perkin-Elmer Tri-Carb 2800TR liquid scintillation counter with 2 mL scintillation fluid (EcoLite, MP Biomedical).

3.6 Ribosome-stimulated GTPase activity of EF-Tu

Nuclotide charging solution containing 4 μM [γ-^{32}P]GTP at 2,000 dpm/pmol, 3 mM PEP, 0.25 mg/mL PK in $TAKM_7$ were pre-incubated at 37°C for 15 min. 0.2 μM

EF-Tu and 0.02 μM EF-Ts were added to the solution and incubated for another 15 min to form the binary complex EF-Tu·[γ-^{32}P]GTP. Ribosomes were programmed by incubating 0.6 μM 70S ribosomes with 1 mg/mL poly(U) mRNA at 37^{o}C for 30 min. The GTP hydrolysis reaction was started upon addition of ribosomes (with or without poly(U)) to the EF-Tu·[γ-^{32}P]GTP binary complex solution. 5 μl samples were taken at various time points, and quenched with 50 μl 1 M $HClO_4$ / 3 mM K_2HPO_4. The released inorganic phosphate (P_i) was extracted by mixing the quenched reaction with 300 μl of 20 mM Na_2MoO_4 and 400 μl of isopropyl acetate for 30 s, and then centrifuged at 11,500 xg for 5 min. 200 μl of the top organic phase from the supernatant was added to 2 mL scintillation fluid (EcoLite, MP Biomedical) and samples were counted in a Perkin-Elmer Tri-Carb 2800TR liquid scintillation counter.

The Mg^{2+} dependence of the ribosome-stimulated GTPase activity of EF-Tu was examined under the same assay conditions described above. However, TAKM buffers with different Mg^{2+} concentrations (3.5 to 10 mM) were used instead of $TAKM_7$.

Kirromycin-stimulated GTPase activity of EF-Tu was examined under the same assay conditions described above. Instead of adding 0.6 μM ribosome to the binary complex solution, 2 μM kirromycin (Sigma) was added. The reaction was quenched with 1 μL 6 M formic acid, and centrifuged at 11,500 xg for 5 min. 1 μL of the supernatant was then spotted on a thin layer chromatography (TLC) PEI Cellulose F (EMD) plastic sheet plate, and developed in 1.5 M K_2HPO_4. The [$^{32}P_i$] and [γ-^{32}P]GTP were detected by phosphor autoradiography imaging using a Typhoon imager (GE Healthcare).

Chapter 4 Results

[1] Part of the chapter was published in De Laurentiis, E.I., Mo, F., and Wieden, H.J. 2011. Construction of a fully active Cys-less elongation factor Tu: functional role of conserved Cysteine 81. *BBA-Proteins and Proteomics* 1814(2011): 684-692

4.1 Functional role of EF-Tu Cys 81

One of the powerful tools to study protein-nucleic acid and protein-protein interactions is fluorescence resonance energy transfer (FRET) between two fluorescent dyes. Specific fluorescent labelling of proteins can be achieved by substituting a residue of choice with Cys, and subsequently modifying the thiol group of the Cysteine side chain with a thiol reactive fluorescent dye.

However, *E. coli* EF-Tu contains three naturally occurring Cysteines, residue 81, 136 and 254. In order to allow for the site specific introduction of the fluorescent dye, all naturally occurring Cys residues need to be removed. Crystal structures of the EF-Tu·GDP complex reveal that one of these three residues (Cys 81) is located near the conserved G2 motif, and that the carbonyl oxygen of Cys 81 is involved in hydrogen-bond interactions with a water molecule that coordinates the Mg^{2+} ion in the nucleotide binding pocket (Song *et al.* 1999) (Figure 4.1). Furthermore, Cys 81 has been found to be highly conserved among bacterial species (89%) and substituted with only two other amino acids, Ala and Met, in some bacteria in nature (De Laurentiis *et al*. 2011). Previous studies have also shown that covalent modification of Cys 81 with *N*-tosyl-L-phenylalanine chloromethane (TPCK) impairs aa-tRNA binding and poly(Phe) synthesis (Jonak *et al.* 1982). In addition, replacing Cys 81 with Gly not only impairs aa-tRNA binding and poly(Phe) synthesis, it also destabilises EF-Tu and causes a decreased affinity for GDP (Anborgh *et al.* 1992). To further study the functional role of Cys 81 and to assess if the Cysteine side chain can be replaced enabling the site-specific introduction of fluorescent and non-fluorescent labels, three versions of a Cysteine-free EF-Tu each containing different amino acid substitution (Ala, Met, Ser) in position 81 as well as Val

in the two non-conserved positions, EF-Tu_{AVV}, EF-Tu_{MVV} and EF-Tu_{SVV}, have been analysed with respect to their guanine nucleotide and ribosome interactions.

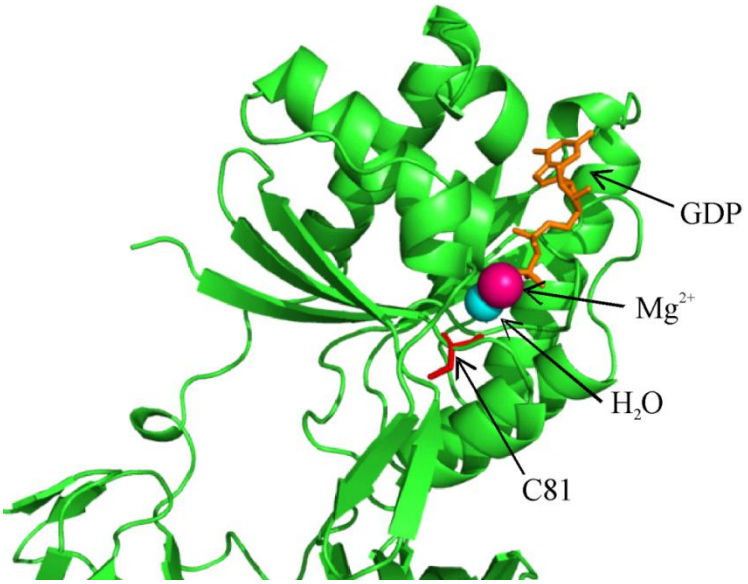

Figure 4.1 Location of Cysteine 81 in the G domain of EF-Tu (PDB: 1EFC). Cys 81 is shown in red stick, the water molecule (cyan) forms a hydrogen bond with both Cys 81 and Mg^{2+} (magenta sphere). GDP is shown in orange.

4.1.1 Guanine nucleotide dissociation

As a G protein, EF-Tu binds to guanine nucleotides; and Cys 81 is located closed to the nucleotide binding pocket. In order to study if substituting Cys 81 affects the nucleotide binding properties, the nucleotide (GDP/GTP) dissociation rate constants for EF-Tu (k_{-1}, k_{-2}) were measured using the stopped-flow technique exploiting FRET from Trp184 in EF-Tu to the mant-group of the respective nucleotide (Figure 4.2). Upon rapid mixing of EF-Tu·mant-nucleotide with excess of unlabelled nucleotide in the stopped-flow apparatus, the release of the mant-nucleotide from EF-Tu resulted in a decrease of mant fluorescence. The respective dissociation rate constant (k_{-1}, k_{-2}) were obtained by

fitting the resulting time course with a one exponential function. As summarised in Table 1, the k_{-1} and k_{-2} values for all mutants were similar to the wild-type values (k_{-1} = 0.002 ± 0.001 s^{-1} and k_{-2} = 0.04 ± 0.01 s^{-1}), suggesting that these three mutations do not alter the guanine nucleotide dissociation properties of EF-Tu.

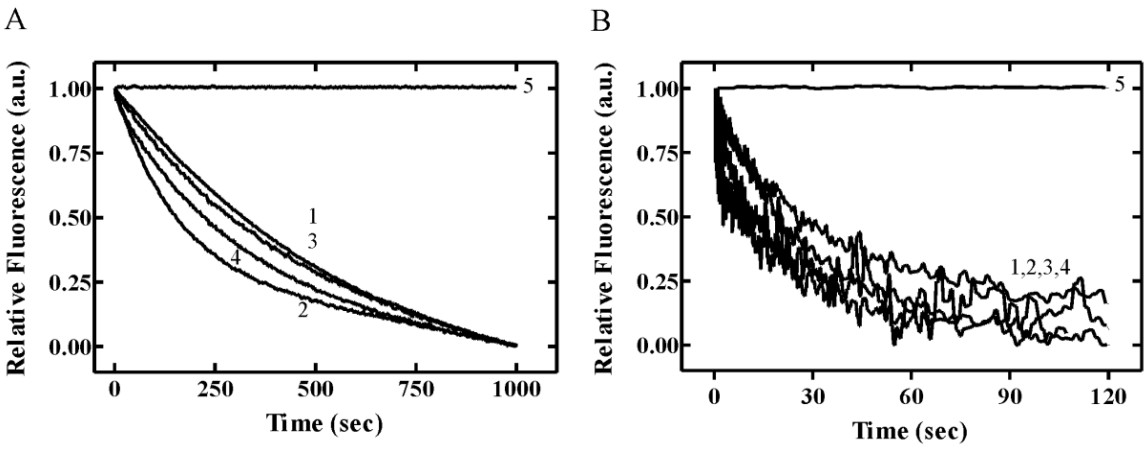

Figure 4.2 Dissociation of GDP/GTP from EF-Tu variants (EF-Tu_{wt}, EF-Tu_{AVV}, EF-Tu_{MVV} and EF-Tu_{SVV}). (A) Time courses of 0.3 μM mant-GDP dissociating from (1) EF-Tu_{wt} (2) EF-Tu_{AVV} (3) EF-Tu_{MVV} (4) EF-Tu_{SVV} (0.3 μM each) was monitored by the emission of mant- fluorescence due to FRET; (5) negative control with only 0.3 μM mant-GDP. (B) The time courses of 0.3 μM mant-GTP dissociating from (1) EF-Tu_{wt} (2) EF-Tu_{AVV} (3) EF-Tu_{MVV} (4) EF-Tu_{SVV} (0.3 μM each) was monitored by the emission of mant-fluorescence exited through FRET; (5) negative control with only 0.3 μM mant-GTP.

Table 1: Dissociation rate constants for GDP and GTP from EF-Tu C81 variants

EF-Tu	GDP dissociation k_{-1} (s^{-1})	GTP dissociation k_{-2} (s^{-1})
EF-Tu_{wt}	0.002 ± 0.001	0.04 ± 0.01
EF-Tu_{AVV}	0.004 ± 0.001	0.06 ± 0.01
EF-Tu_{MVV}	0.002 ± 0.001	0.04 ± 0.01
EF-Tu_{SVV}	0.003 ± 0.001	0.06 ± 0.01

4.1.2 Guanine nucleotide association

The association rate constants for GDP and GTP binding to EF-Tu (k_1 and k_2, respectively) were determined using a constant concentration of nucleotide free EF-Tu and varying concentrations of mant-GDP or mant-GTP. Upon binding of the mant-labelled nucleotide to EF-Tu, an increase of mant-fluorescence was observed (Figure 4.3 A and B). Apparent rate constant (k_{app}) values for each titration point were determined by fitting the time course with a single-exponential equation. The concentration dependence of k_{app} can then be plotted as a function of the mant-nucleotide concentration yieded k_1 and k_2 from the slope of the linear fit (Figure 4.3 C and D). The value for k_{-1} and k_{-2} can be determined from the respective y-axis intercept, which was closed to zero (Table 2).

Compared to the wild-type GDP association rate constant of $k_1 = (1.6 \pm 0.2) \times 10^6$ $M^{-1}s^{-1}$, the EF-Tu_{MVV} variant showed a three-fold increase in the k_1 value, whereas the other two variants behaved similar to the wild-type. On the other hand, EF-Tu_{AVV} showed a two-fold decrease in the k_2 value, when compared to the other two variants and the wild-type with an association rate constant of $k_2 = (3.7 \pm 0.2) \times 10^5$ $M^{-1}s^{-1}$ for GTP.

Equilibrium binding constant (K_D) values for each EF-Tu variant were calculated from nucleotide dissociation and association rate constants ($K_D = k_{-1}/k_1$, values are summarized in Table 3). Compared to the wild-type K_D values, a three-fold increase of the equilibrium binding constant for the respective mutants was observed.

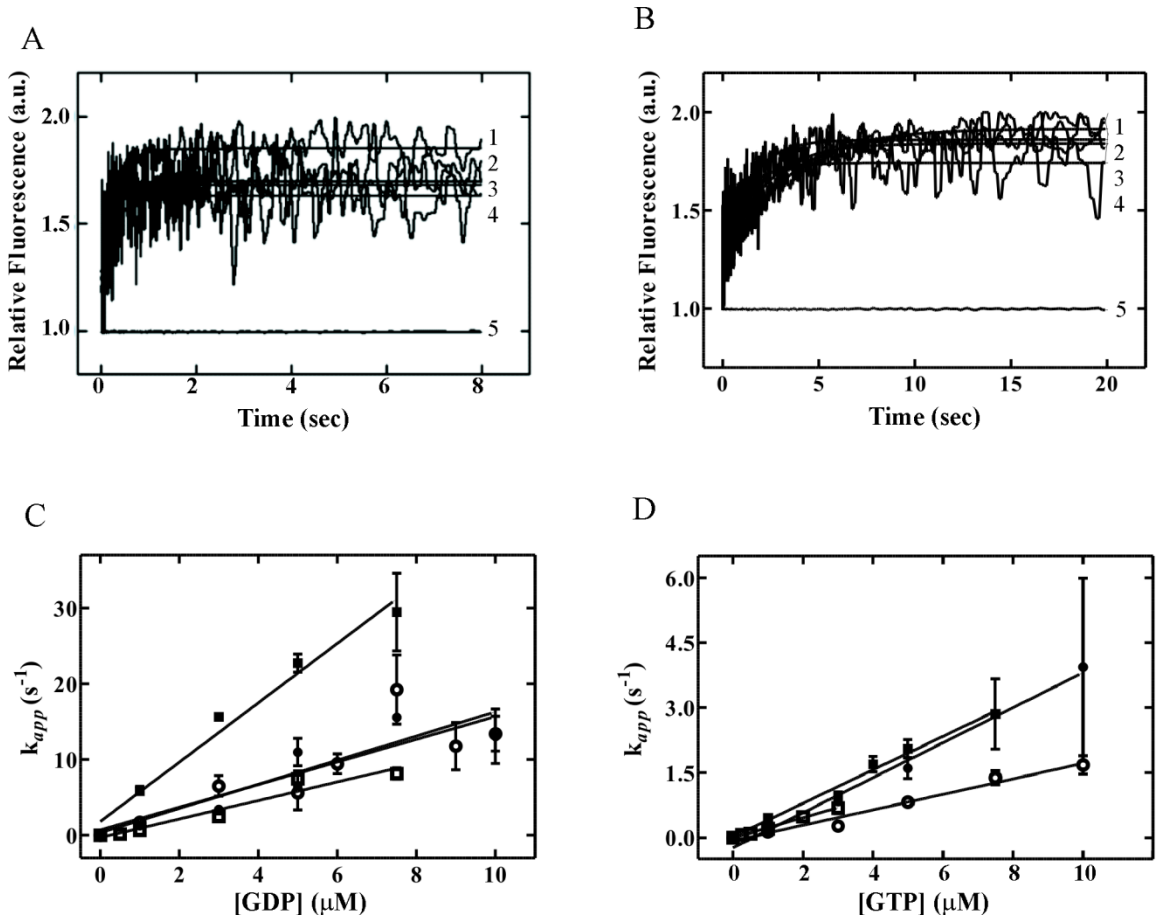

Figure 4.3 Association of GDP and GTP with EF-Tu C81 variants. (A) Time courses of 3 μM mant-GDP associating with (1) EF-Tu_{wt} (2) EF-Tu_{AVV} (3) EF-Tu_{MVV} (4) EF-Tu_{SVV} (0.3 μM each) was monitored by the emission of mant- fluorescence from FRET; (5) negative control with only 3 μM mant-GDP. (B) Time courses of 3 μM mant-GTP associating with (1) EF-Tu_{wt} (2) EF-Tu_{AVV} (3) EF-Tu_{MVV} (4) EF-Tu_{SVV} (0.3 μM each) was monitored by the emission of mant- fluorescence from FRET; (5) negative control with only 3 μM mant-GTP. (C) and (D) concentration dependent of k_{app} calculated by fitting time course in (A) and (B) with one exponential function. (●) EF-Tu_{wt}; (○) EF-Tu_{AVV}; (■) EF-Tu_{MVV}; (□) EF-Tu_{SVV}.

Table 2: Association rate constants of GDP and GTP with EF-Tu C81 variants

EF-Tu	GDP association k_1 ($M^{-1}s^{-1}$)	GTP association k_2 ($M^{-1}s^{-1}$)
$EF\text{-}Tu_{wt}$	$(1.6 \pm 0.2) \times 10^6$	$(3.7 \pm 0.2) \times 10^5$
$EF\text{-}Tu_{AVV}$	$(1.6 \pm 0.2) \times 10^6$	$(1.7 \pm 0.1) \times 10^5$
$EF\text{-}Tu_{MVV}$	$(4.3 \pm 0.2) \times 10^6$	$(3.9 \pm 0.1) \times 10^5$
$EF\text{-}Tu_{SVV}$	$(1.2 \pm 0.2) \times 10^6$	$(2.2 \pm 0.1) \times 10^5$

Table 3: Summary of the equilibrium binding constants of GDP and GTP with EF-Tu C81 variants

EF-Tu	K_D GDP (nM)	K_D GTP (nM)
$EF\text{-}Tu_{wt}$	1.3 ± 0.8	110 ± 30
$EF\text{-}Tu_{AVV}$	3.0 ± 1.0	350 ± 80
$EF\text{-}Tu_{MVV}$	0.5 ± 0.1	100 ± 30
$EF\text{-}Tu_{SVV}$	3.0 ± 1.0	270 ± 60

4.1.3 Interaction of mutant EF-Tu with EF-Ts

In order to study the effect that substituting Cys 81 with Ala, Met and Ser has on the interaction between EF-Tu and the nucleotide exchange factor EF-Ts, EF-Ts-induced nucleotide dissociation was measured by monitoring the fluorescence of mant-GDP and mant-GTP dissociation from EF-Tu in the presence of EF-Ts. In this case, after rapidly mixing EF-Tu·mant-GDP or EF-Tu·mant-GTP with excess unlabelled nucleotide in the presence of EF-Ts, a rapid decrease in mant-fluorescence was observed due to the release of bound mant-nucleotide (Figure 4.4). The rates of nucleotide dissociations were determined from the time course by fitting with a single-exponential equation. As

summarized in Table 4, all EF-Tu variants showed similar rates for EF-Ts-induced GDP and GTP dissociation ($k_{appTs.GDP}$ and $k_{appTs.GTP}$, respectively) when compared to the wild-type values which are $k_{appTs.GDP} = 2.6 \pm 0.1\ s^{-1}$ and $k_{appTs.GTP} = 6.9 \pm 0.1\ s^{-1}$. These results demonstrate that the three introduced Cys81 substitutions do not affect the binding of EF-Ts for EF-Tu nor do they alter the exchange mechanism, since similar dissociation rates were observed for mutants and wilde-type EF-Tu in the presence of the same concentration of EF-Ts.

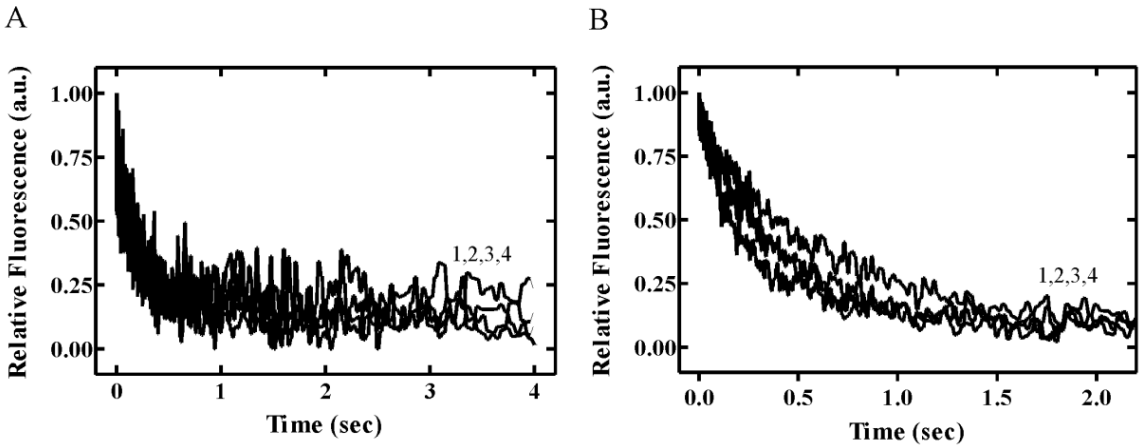

Figure 4.4 EF-Ts-stimulated dissociation of GDP and GTP from EF-Tu C81 variants. (A) Time courses of 0.3 μM mant-GDP dissociating from (1) EF-Tu_{wt} (2) EF-Tu_{AVV} (3) EF-Tu_{MVV} (4) EF-Tu_{SVV} (0.3 μM each) in the presence of 1μM EF-Ts was monitored by the emission of mant- fluorescence due to FRET. (B) Time courses of 0.3 μM mant-GTP dissociating from (1) EF-Tu_{wt} (2) EF-Tu_{AVV} (3) EF-Tu_{MVV} (4) EF-Tu_{SVV} (0.3 μM each) in the presence of 1μM EF-Ts was monitored by the emission of mant-fluorescence due to FRET.

Table 4: EF-Ts stimulated nucleotide dissociation from EF-Tu C81 variants

EF-Tu	GDP dissociation $k_{appTs.GDP}$ (s^{-1})	GTP dissociation $k_{appTs.GTP}$ (s^{-1})
$EF\text{-}Tu_{wt}$	2.6 ± 0.1	6.9 ± 0.1
$EF\text{-}Tu_{AVV}$	4.4 ± 0.1	6.3 ± 0.1
$EF\text{-}Tu_{MVV}$	2.5 ± 0.1	7.1 ± 0.1
$EF\text{-}Tu_{SVV}$	1.7 ± 0.1	4.9 ± 0.1

4.1.4 Dipeptide formation

During the elongation cycle of protein synthesis, EF-Tu·GTP delivers aa-tRNA to the mRNA programmed ribosome. De Laurentiis and co-workers have shown that the mutants $EF\text{-}Tu_{MVV}$ and $EF\text{-}Tu_{SVV}$ have a significant reduced ability to protect the aminoacyl-ester bond of the aa-tRNA against spontaneously hydrolysis, while $EF\text{-}Tu_{AVV}$ has similar activity as the wild-type (De Laurentiis *et al.* 2011) (Table 5).

In order to examine the ability of EF-Tu variants to deliver aa-tRNA to the ribosome and to assess if all ribosome-dependent steps can occur, a dipeptide formation assay was performed. Wild-type as well as mutant EF-Tu was first charged with GTP, then [^{14}C] $Phe\text{-}tRNA^{Phe}$ was added to form the ternary complex. 70S ribosome was programmed with the synthetic poly(U) mRNA, which codes for amino acid Phe, and then incubated with [^{14}C] $Phe\text{-}tRNA^{Phe}$. For dipeptide formation, the ternary complex was incubated with poly(U)-programmed ribosomes for 30 s, and dipeptides were separated using HPLC. The percent yield of dipeptides formed was calculated from the respective amount of [^{14}C] found in the Phe-Phe dipeptide peak. As shown in Figure 4.5,

all mutants behaved like the wild-type with dipeptide formation values closed to 100% under these conditions.

Table 5: EF-Tu protection against spontaneous hydrolysis of Phe-tRNA^{Phe} (De Laurentiis *et al.* 2011)

EF-Tu	$t_{1/2}$ Phe-tRNA^{Phe} (min)
EF-Tu$_{wt}$	90 ± 5
EF-Tu$_{AVV}$	79 ± 19
EF-Tu$_{MVV}$	37 ± 4
EF-Tu$_{SVV}$	34 ± 8
no EF-Tu	10 ± 7

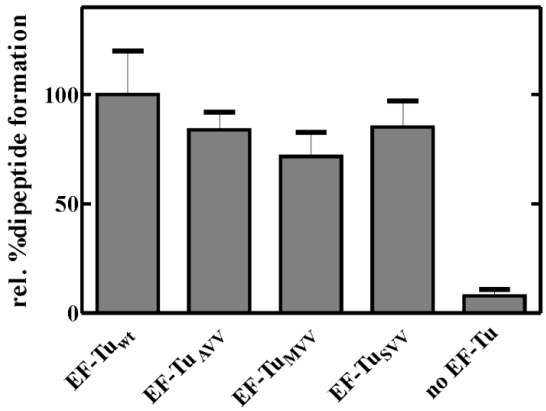

Figure 4.5 Percentage of dipeptide formed relative to the EF-Tu$_{wt}$ activity. [^{14}C]Phe-[^{14}C]Phe peptide bond formation within 30 s was measured in the presence of EF-Tu variants at 10 mM Mg^{2+}. Dipeptides formed were separated using HPLC and quantified by scintillation counting.

4.1.5 Ribosome-stimulated EF-Tu GTPase activity

During protein synthesis, EF-Tu·GTP delivers aa-tRNA to the ribosome. Upon codon-anticodon recognition, EF-Tu hydrolyzes GTP to GDP and changes its conformation to the GDP-bound form. It has been shown that the ribosome can stimulate the GTPase activity of EF-Tu even in the absence of aa-tRNA, but to a very much lower extent (Donner *et al.* 1978). The ability of the mutant EF-Tus to hydrolyze GTP in the presence of ribosome, but in the absence of aa-tRNA was examined and compared to the wild-type. EF-Tu and EF-Ts were incubated with [γ-^{32}P]GTP, and the reaction was started upon the addition of ribosomes. Aliquots of the reaction were taken at different time points. The released [$^{32}P_i$] was extracted and measured by liquid scintillation counting. The intrinsic GTPase activity of EF-Tu is extremely low and could not be determined under these conditions. As shown in Figure 4.6, the GTPase activity of EF-Tu_{wt} was strongly stimulated by the presence of 70S ribosome (0.06 pmol GTP hydrolyzed per min); however, EF-Tu_{MVV} showed 4 times less of the activity and, interestingly, both the EF-Tu_{AVV} and EF-Tu_{SVV} showed an even more reduced activity.

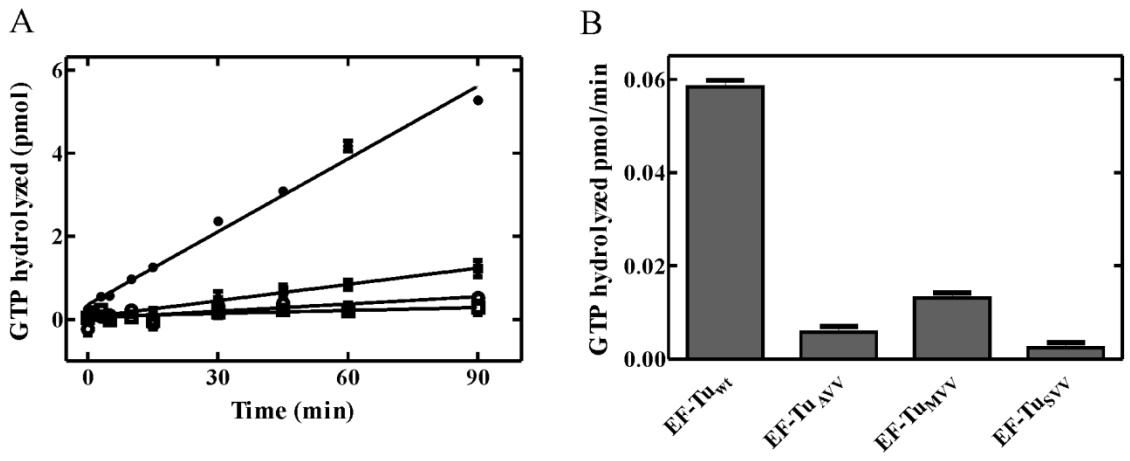

Figure 4.6 70S Ribosome-stimulated EF-Tu GTPase activity. (A) pmol GTP hydrolyzed over time of EF-Tu was measured by reacting 0.2 μM EF-Tu, 0.02 μM EF-Ts and 4 μM [γ- ^{32}P]GTP with 0.6 μM 70S ribosomes. The reaction was quenched after various time points and the released inorganic phosphate was extracted and quantified by scintillation counting. (●) EF-Tu$_{wt}$; (○) EF-Tu$_{AVV}$; (■) EF-Tu$_{MVV}$; (□) EF-Tu$_{SVV}$. (B) Rate of ribosome-stimulated GTP hydrolysis of EF-Tu variants. The rate of GTP hydrolysis by EF-Tu variants was obtained by fitting time courses in (A) with a linear equation.

4.2 EF-Tu Domain II variants

During protein synthesis EF-Tu not only interacts with aa-tRNA but also with the ribosome. During the elongation cycle, EF-Tu·GTP·aa-tRNA binds to the ribosomal A-site, and following codon recognition the GTPase activity of EF-Tu is stimulated. The details of how the signal is transmitted from the ribosomal decoding site to EF-Tu are still unknown, but it has been suggested that the interactions between the ternary complex and the ribosome indirectly induce or stabilize conformational transitions in EF-Tu during GTP hydrolysis (Rodnina *et al.* 2005). Several groups reported cryo-EM structures and revealed that domain II of EF-Tu forms a contact with helix 5 of the 23S rRNA during A-site binding (Stark *et al.* 2002; Valle *et al.* 2002). More recent X-ray structures suggest that residues 221 and 222 in EF-Tu domain II interact with 16S rRNA bases 55, 56 and 368, as well as that EF-Tu residues 278 to 281 interact with 16S rRNA

bases 367 and 368 through hydrophobic interaction and hydrogen bonding (Schmeing *et al.* 2009; Schuette *et al.* 2009). More importantly, four of the seven residues in EF-Tu between positions 219 and 226 are more than 99% conserved in all species; and the hydrogen bonding interaction between Arg 279 and U368 is 99.7% conserved across all species (Schmeing *et al.* 2009) (Figure 4.7). Previous biochemical studies demonstrated that the substitution of Gly 222 with Asp inhibits the ribosome-stimulated GTP hydrolysis by EF-Tu, preventing protein synthesis. Interestingly, this effect can be overcome by higher Mg^{2+} concentration (10 mM). However, it is not clear if an alternative signalling pathway is used (Vorstenbosch *et al.* 1996). Furthermore, replacing Gly 280 with Val resulted in a ternary complex impaired in binding to the ribosome and reduced protein synthesis rates, consequently, expression of the mutant *tuf gene* alone cannot support cell growth (Tubulekas and Hughes 1993). More interestingly, the antibiotic kirromycin has been found to inhibit protein synthesis by blocking the release of the EF-Tu·GDP complex from the ribosome after aa-tRNA binding and GTP hydrolysis (Wolf *et al.* 1974), but kirromycin cannot block the ternary complex containing EF-Tu G280V on the ribosome (Tubulekas and Hughes 1993). In order to investigate the functional role of amino acids around G280 for the regulation of the GTPase activity of EF-Tu, three mutant EF-Tus containing R279A, G280V or R283A were constructed (Figure 4.8), and their activity with respect to their interaction with guanine nucleotide and the ribosome was analyzed.

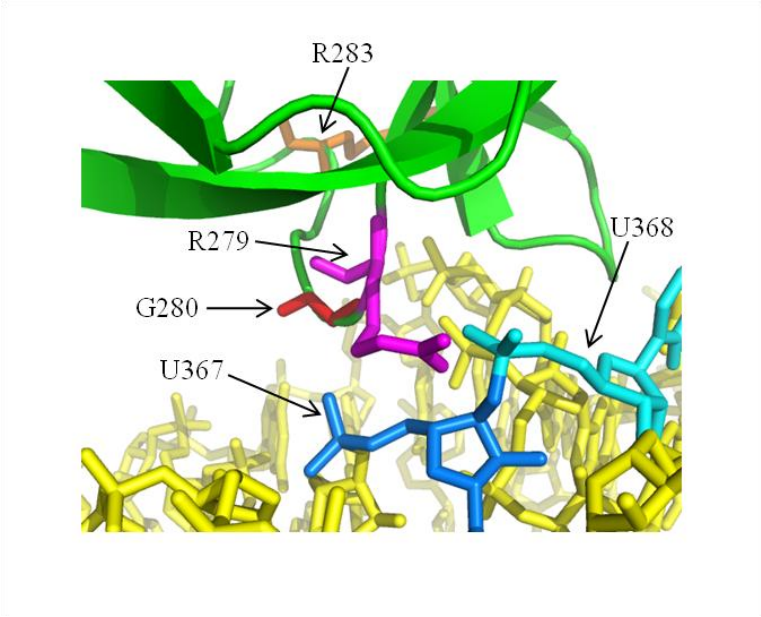

Figure 4.7 Interaction of R279 in EF-Tu with 16S rRNA U368 in 30S ribosomal subunit (PDB: 3FIN). R279 is shown in magenta and 23S rRNA U368 in cyan.

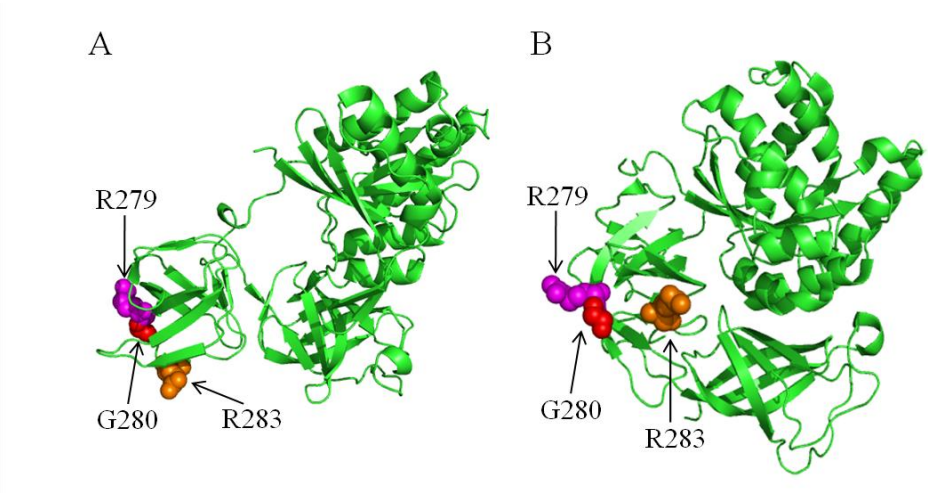

Figure 4.8 Structure comparison of residues R279, G280 and R283 in EF-Tu in two conformations. Cartoon diagram of *Escherichia coli* EF-Tu·GDP (A) (PDB: 1EFC) and *Thermus thermophilus* EF-Tu·GTP (B) (PDB: 1EXM). R279 is shown in magenta, G280 in red, and R283 in orange.

4.2.1 Guanine nucleotide dissociation

The nucleotide GDP and GTP dissociation rate constants (k_{-1}, k_{-2}) were determined as described in the material and methods section and are summarized in Table 6. When compared to the respective wild-type values of $k_{-1} = 0.002 \pm 0.001\ s^{-1}$ and $k_{-2} = 0.04 \pm 0.01\ s^{-1}$, all EF-Tu variants showed similar behaviour, except for EF-Tu_{R279A} which showed a four-fold decrease in the GTP dissociation rate constant.

Table 6: Dissociation rates constants for GDP and GTP from EF-Tu domain II variants

EF-Tu	GDP dissociation k_{-1} (s^{-1})	GTP dissociation k_{-2} (s^{-1})
EF-Tu_{wt}	0.002 ± 0.001	0.04 ± 0.01
EF-Tu_{R279A}	0.002 ± 0.001	0.01 ± 0.01
EF-Tu_{G280V}	0.003 ± 0.001	0.03 ± 0.01
EF-Tu_{R283A}	0.002 ± 0.001	0.05 ± 0.01

4.2.2 Guanine nucleotide association

GDP and GTP binding to EF-Tu were studied using the same method as for the EF-Tu Cys81 mutants. Time courses were fit to a single-exponential function (Figure 4.9), and the nucleotide association constants are summarized in Table 7. When compared to the wild-type values of $k_1 = (1.6 \pm 0.2) \times 10^6\ M^{-1}s^{-1}$ and $k_2 = (3.7 \pm 0.2) \times 10^5\ M^{-1}s^{-1}$, all mutant proteins showed similar behaviour, except EF-Tu_{G280V} which showed a three-fold increase in the GDP association rate constant (k_1). Equilibrium binding constant (K_D) values for each EF-Tu variant were calculated from the respective nucleotide dissociation

(k_{-1}/k_{-2}) and association rate constants (k_1/k_2), and are summarized in Table 8. Compared to EF-Tu wild-type (K_D GDP = 1.3 ± 0.8 nM and K_D GTP = 110 ± 30 nM), all EF-Tu variants showed similar values within the standard deviation.

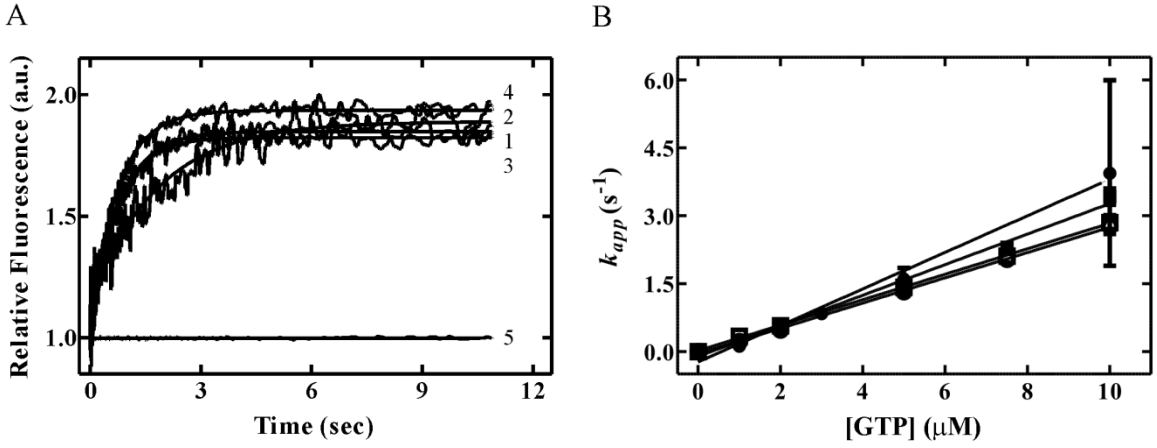

Figure 4.9 Association of GTP with EF-Tu domain II variants. (A) Time courses of 3 μM mant-GTP binding to (1) EF-Tu_{wt} (2) EF-Tu_{R279A} (3) EF-Tu_{G280V} (4) EF-Tu_{R283A} (0.3 μM each) was monitored by the emission of mant- fluorescence caused by FRET; (5) negative control with only 3 μM mant-GTP. (B) Concentration dependence of the k_{app}s calculated by fitting time courses in (A) with a single-exponential function. (●) EF-Tu_{wt}; (○) EF-Tu_{R279A}; (■) EF-Tu_{G280V}; (□) EF-Tu_{R283A}.

Table 7: Association rate constants of GDP and GTP with EF-Tu domain II variants

EF-Tu	GDP association k_1 ($M^{-1}s^{-1}$)	GTP association k_2 ($M^{-1}s^{-1}$)
EF-Tu_{wt}	(1.6 ± 0.2) x 10^6	(3.7 ± 0.2) x 10^5
EF-Tu_{R279A}	(1.4 ± 0.1) x 10^6	(2.8 ± 0.1) x 10^5
EF-Tu_{G280V}	(4.3 ± 0.5) x 10^6	(3.5 ± 0.1) x 10^5
EF-Tu_{R283A}	(2.4 ± 0.2) x 10^6	(2.7 ± 0.1) x 10^5

Table 8: Summary of the equilibrium binding constants of GDP and GTP with EF-Tu domain II variants

EF-Tu	K_D GDP (nM)	K_D GTP (nM)
$EF\text{-}Tu_{wt}$	1.3 ± 0.8	110 ± 30
$EF\text{-}Tu_{R279A}$	1.4 ± 0.7	40 ± 30
$EF\text{-}Tu_{G280V}$	0.5 ± 0.2	85 ± 30
$EF\text{-}Tu_{R283A}$	0.8 ± 0.4	185 ± 40

4.2.3 Interaction of EF-Tu domain II variants with EF-Ts

In the crystal structure of EF-Tu, residues R279, G280 and R283 are located on the surface of domain II, and do not interact with either the nucleotide binding pocket of domain I or the EF-Ts binding site, suggesting that mutations in these positions should not affect the nucleotide-binding or exchanging properties of the protein (PDB:1TTT and 1EFU) (Nissen *et al.* 1995; Kawashima *et al.* 1996). To confirm this, the effect of the domain II mutations on the interaction between EF-Tu and its nucleotide exchange factor EF-Ts were determined. EF-Ts-induced nucleotide dissociation was measured by monitoring the fluorescence change upon mant-GDP and mant-GTP dissociation from EF-Tu in the presence of a fixed amount of EF-Ts. When EF-Tu·mant-GDP or mant-GTP was rapidly mixed with excess unlabelled nucleotide in the presence of EF-Ts, a decrease in mant fluorescence due to the release of mant-GDP or mant-GTP was observed. The rates of nucleotide dissociation were determined from the observed time courses by fitting with a single-exponential equation. Table 9 summarizes the apparent rate constants ($k_{appTs.GDP}$ and $k_{appTs.GTP}$) for GDP and GTP dissociation. Compared to wild-type EF-Tu

GDP-dissociation rate $k_{appTs.GTP}$ = 2.6 ± 0.1 s^{-1}, and GTP-dissociation rate $k_{appTs.GTP}$ = 6.9 ± 0.1 s^{-1}, all EF-Tu variants showed two or three-fold increases in the respective values.

Table 9: EF-Ts stimulated nucleotide dissociation from the EF-Tu domain II variants.

EF-Tu	GDP dissociation $k_{Ts.GDP}$ (s^{-1})	GTP dissociation $k_{Ts.GTP}$ (s^{-1})
$EF\text{-}Tu_{wt}$	2.6 ± 0.1	6.9 ± 0.1
$EF\text{-}Tu_{R279A}$	1.4 ± 0.1	18 ± 0.1
$EF\text{-}Tu_{G280V}$	0.7 ± 0.1	11 ± 0.1
$EF\text{-}Tu_{R283A}$	0.8 ± 0.1	13 ± 0.1

4.2.4 70S ribosome- and kirromycin-stimulated EF-Tu GTP hydrolysis

Residue R279 in EF-Tu has been shown to interact with the backbone of helix 15 of the16S rRNA of the 30S ribosomal subunit (Schuette *et al.* 2009) and, therefore, could play a role in the signalling pathway of GTPase activation in EF-Tu. Furthermore, the substitution of G280V has been shown to impair GTPase activation of EF-Tu on the ribosome (Tubulekas and Hughes 1993). To verify the results concerning the substitution of G280V and to analyze the effect of the substitution of R279A, R283A on EF-Tu, the ability of EF-Tu variants to hydrolyze GTP in the presence of unprogrammed 70S ribosomes and poly(U)-programmed 70S ribosomes were examined. As shown in Figure 4.10, the GTPase activity of EF-Tu variants in the presence of 70S ribosome and poly(U) programmed 70S ribosome were identical. However, wild-type EF-Tu was strongly

stimulated by the presence of 70S ribosome and hydrolyzed 0.1 pmol GTP per min, but all EF-Tu variants showed reduced activity.

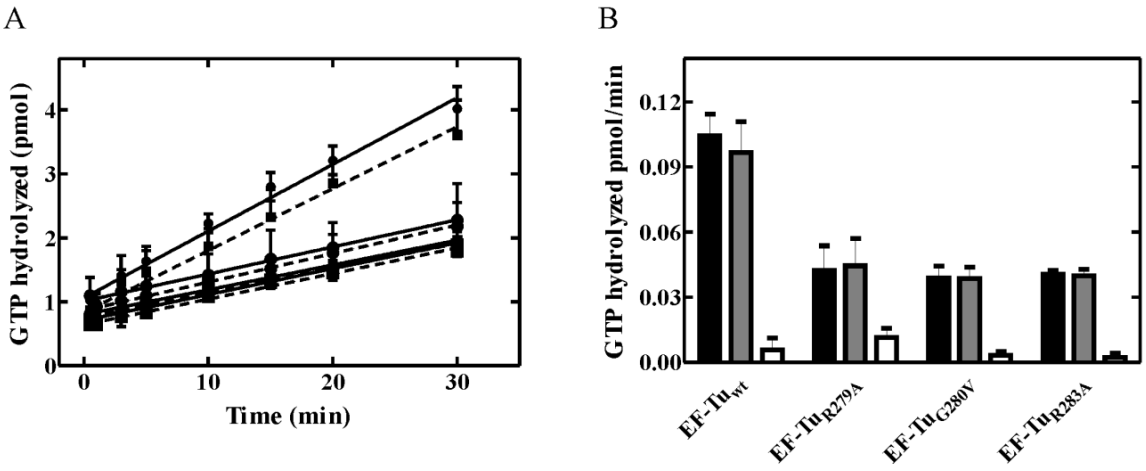

Figure 4.10 70S Ribosome-stimulated EF-Tu variants GTPase activity. (A) GTP hydrolysis by EF-Tu was measured by reacting 0.2 μM EF-Tu, 0.02 μM EF-Ts and 4 μM [γ- ^{32}P]GTP with 0.6 μM unprogrammed 70S ribosome (solid line) or poly(U)-programmed ribosome (dash line). The reaction was quenched after various time points and the released inorganic phosphate was extracted and quantified by scintillation counting. (●) EF-Tu$_{wt}$; (○) EF-Tu$_{R279A}$; (■) EF-Tu$_{G280V}$; (□) EF-Tu$_{R283A}$. (B) Summary of GTPase activity of EF-Tu variants, poly(U)-programmed ribosome (black), empty 70S ribosome (grey) and without ribosome (white). The rate of GTP hydrolysis by EF-Tu variants was obtained by fitting time course in (A) with a linear equation, and the slope of the linear fit represents the rate of GTP hydrolysis.

The antibiotic kirromycin has been reported to efficiently inhibit polypeptide synthesis by blocking the release of EF-Tu from the translating ribosome (Wolf *et al*. 1974; Wolf *et al*. 1977). However, kirromycin can induce EF-Tu's GTPase activity in the absence of aa-tRNA and ribosome (Chinali *et al*. 1977). Interestingly, while substitution of EF-Tu G280 to Val resulted in reduced translation efficiency, kirromycin could not inhibit protein synthesis by binding to this mutant EF-Tu, suggesting that G280 in EF-Tu plays an important role in the interaction of the ternary complex with the ribosome, such

as altering EF-Tu conformation during ribosomal A-site binding (Tubulekas and Hughes 1993). Thus, both the unprogrammed ribosome- and kirromycin-stimulated EF-Tu GTPase activity were measured and compared. As shown in Figure 4.11, the three EF-Tu variants showed at least a three-fold decrease in the ribosome-stimulated activity, but kirromycin can stimulate the activity to almost the same extend. These results suggested that substitution of these three residues do not disrupt EF-Tu's GTPase machanism, and these residues are important for the interaction of EF-Tu and the ribosome during protein synthesis.

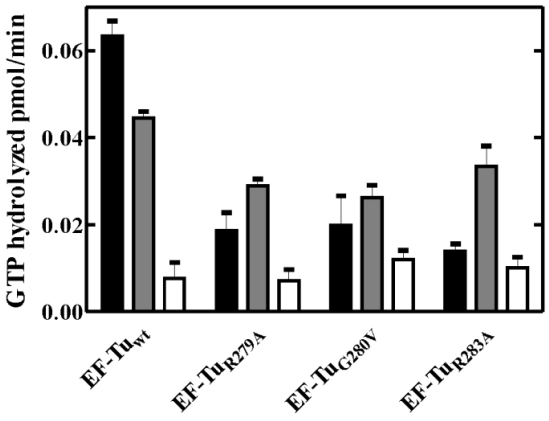

Figure 4.11 Ribosome- and kirromycin-stimulated EF-Tu GTPase activity. Summary of GTPase activity of EF-Tu variants. The reaction was quenched after various time points and the released inorganic phosphate were quantified by TLC. The rate of GTP hydrolysis by EF-Tu variants was obtained by fitting time course of GTP hydrolyzed over time with a linear equation, and the slope of the linear fit represents the rate of GTP hydrolysis. EF-Tu·GTP with 70S ribosome (black), with kirromycin (grey), without ribosome and kirromycin (white).

The structural flexibility of RNA and proteins in the 70S ribosome depend on the Mg^{2+} concentration (Yamamoto *et al.* 2010). Therefore, in order to test if higher Mg^{2+}

concentration can rescue EF-Tu variants' GTPase activity, Mg^{2+} dependence of the GTPase activities of EF-Tu variants was measured at different Mg^{2+} concentrations. As shown in Figure 4.12, $EF\text{-}Tu_{wt}$ always shows a higher GTPase activity than EF-Tu variants regardless of the Mg^{2+} concentration. All EF-Tu variants and the wild-type showed the lowest activity at 3.5 mM Mg^{2+}, and similar activities in the range of 5-10 mM Mg^{2+}.

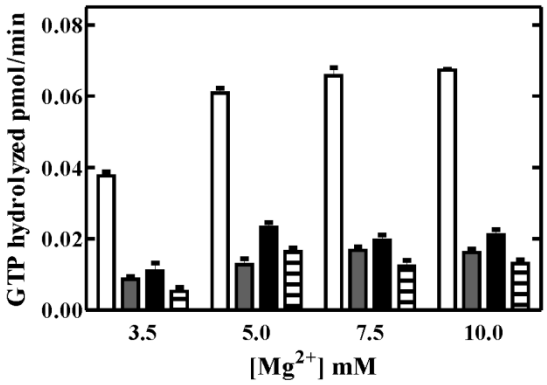

Figure 4.12 Mg^{2+} dependence of 70S ribosome-stimulated EF-Tu GTPase activity. Rate of GTP hydrolysis by EF-Tu was measured by reacting 0.2 μM EF-Tu, 0.02 μM EF-Ts and 4 μM [γ- ^{32}P]GTP with 0.6 μM 70S ribosome at different Mg^{2+} concentration. The reaction was quenched after various time points and the released inorganic phosphate was extracted and quantified by scintillation counting. The rate of GTP hydrolysis by EF-Tu variants was obtained by fitting time course of GTP hydrolyzed over time with a linear equation, and the slope of the linear fit represents the rate of GTP hydrolysis. $EF\text{-}Tu_{wt}$ (white); $EF\text{-}Tu_{R279A}$ (grey); $EF\text{-}Tu_{G280V}$ (black); $EF\text{-}Tu_{R283A}$ (striped).

4. 3 Summary

In summary, substitution of Cys 81 with Ala, Met and Ser does not affect the nucleotide binding properties and the EF-Ts catalyzed nucleotide exchange mechanism of EF-Tu, but EF-Tu variants with Met and Ser showed reduced ability to protect

spontaneously hydrolysis of the aminoacyl ester bond of the aa-tRNA. Although these mutant proteins can deliver aa-tRNA to the ribosome and form dipeptides like the wild-type protein under the assay condition, all proteins showed a significantly reduced ability to hydrolyze GTP in the presence of the ribosome. When compared to wild-type EF-Tu, the mutant proteins containing R279A, G280V or R283A have the same affinity for the guanine nucleotide, but showed reduced ability to hydrolyze GTP in the presence of the ribosome under the multiple turnover condition and different Mg^{2+} concentrations. However, the antibiotic kirromycin can stimulate their GTPase activity to the same extent as for the wild-type protein.

Chapter 5 Discussion

5.1 Functional role of EF-Tu Cys 81

The elongation factor Tu is one of the most abundant proteins in all living cells, and it is well conserved among the three domains of lives (Chiron *et al.* 2005). The interaction between EF-Tu, GTP, aa-tRNA and the ribosome has been studied in bacteria through crystal structures and biochemical assays for decades (Ramakrishnan 2002). Although kinetic studies have revealed several individual steps during protein synthesis, little is known about the dynamics of the whole process including how or when proteins change their conformation or how or when the signal travels between or within each participating macromolecule.

One of the methods to study the interaction between biomolecules is through fluorescently labelled compounds. Due to the rarity of Cystetine in proteins and its special properties, normally a Cysteine is introduced at an interesting position on the surface of the protein, enabling the chemical modification with a fluorescent reporter group (Kim *et al.* 2008). In order to label *E. coli* EF-Tu at a specific position on the molecular surface using Cysteine as a linker, it is necessary to remove all Cysteines present in wild-type EF-Tu to create a Cys-free elongation factor. *E. coli* EF-Tu contains three Cysteines, Cys 81, Cys 136 and Cys 254. Two of these residues (Cys 136 and Cys 254) were replaced by Valine, which is the most commonly found amino acid substitution at these positions, with degree of substitution of 37% and 31%, respectively. Only Cys 81 is highly conserved among 125 bacterial species and was found to be substituted with Alanine (10%) and Methionine (1%) in nature (De Laurentiis *et al.* 2011). Previous studies have shown that Cys 81 can be modified with *N*-tosyl-L-phenylalanyl chloromethane (TPCK) and that this modification impaired aa-tRNA binding and

poly(Phe) synthesis (Jonak *et al.* 1982). This raised the question what the functional role of Cys 81 in EF-Tu is during protein synthesis, and if it is possible to substitute Cys 81 in EF-Tu.

To study the functional role of Cys 81, Anborgh and co-workers constructed a Glycine substitution variant (Anborgh *et al.* 1992). This study revealed that introducing Glycine in position 81 of EF-Tu leads to destabilization of the protein, a 13-fold increase of the K_D for GDP, an impaired aa-tRNA binding and a reduced activity during poly(Phe) synthesis (Anborgh *et al.* 1992). This severe impact on the function of EF-Tu is consistent with the sequence alignment reported by De Laurentiis *et al.* 2011, where no Glycine could be found as substituent at position 81. This study also showed that Alanine and Methionine are common substitutions at this position in bacteria, suggesting that these substitutions may not affect the function of EF-Tu. Interestingly, although Serine is structurally similar to Cystein and, therefore, a potential conservative substitution for Cys 81, it is not found in the sequence of 125 bacterial EF-Tu (De Laurentiis *et al.* 2011).

Here, the three Cys-less EF-Tu variants: EF-Tu_{AVV}, EF-Tu_{MVV} and EF-Tu_{SVV} were analyzed and revealed that the introduced substitutions do not affect the nucleotide binding property of EF-Tu, nor the interaction between EF-Tu and EF-Ts. However, while EF-Tu_{AVV} could protect the spontaneous hydrolysis of the aminoacyl ester bond of the aa-tRNA similar to the wild-type, EF-Tu_{MVV} and EF-Tu_{SVV} showed 3 times reduced protection. Moreover, none of the variants had a strong affect on the EF-Tu mediated aa-tRNA binding and subsequent peptide bond formation under the assay conditions, which suggests that EF-Tu variants can bind aa-tRNA and deliver it to the ribosome. However, all EF-Tu variants showed a significant reduced aa-tRNA independent ribosome-

stimulated GTPase activity, which suggests that Cys 81 may play an important role in EF-Tu's GTPase activation.

5.1.1 Guanine nucleotide binding properties

Mg^{2+} is an essential cofactor in the GTPase reaction of all guanine nucleotide-binding proteins (Gilman 1987). EF-Tu Cys 81 is located close to the nucleotide binding pocket and its backbone carbonyl oxygen forms a hydrogen bond with a water molecule which positions the Mg^{2+} ion at the nucleotide in the nucleotide binding pocket (Song *et al.* 1999). Anborgh *et al.* showed that substitution of Cys 81 to Gly increases the GDP dissociation rate and induces destabilization of the protein, suggesting that Cys 81 is involved in the ability of EF-Tu to discriminate between GDP and GTP, and that Cys 81 is an important stabilizing element in the architecture of the guanine-nucleotide-binding region (Anborgh *et al.* 1992). Moreover, Glycine has a side chain with one single hydrogen atom, while Alanine, Methionine and Serine have either similar or longer side chain than Cysteine. By substituting Cys with Gly, an increase of flexibility of the backbone atoms may break the interaction between the water molecule and the carbonyl oxygen of Cys 81. Hence, the contribution of Cys 81 to the ability of EF-Tu to discriminate between GDP and GTP may not be determined by a specific amino acid at this position, but may be a result of the flexibility of backbone atoms and their interaction with water molecules. The determination of the kinetic parameters governing the interaction between the two guanine nucleotides and EF-Tu reported here demonstrate that replacing Cysteine with side chains of different sizes does not significantly affect nucleotide binding. This supports the notion that increased flexibility in position 81 might be the cause for the observed lowered affinity for GDP in the reported C81G variant.

However, it does not explain the evolutionary pressure on position 81 selecting for Cysteine in this position as the Serine mutant exhibit wild-type like behaviour suggesting a critical role of Cys 81 in a different functional property of EF-Tu.

5.1.2 aa-tRNA binding property and peptide formation

Aminoacyl-tRNA plays a central role in protein synthesis by delivering the amino acid that corresponds to the mRNA codon displayed in the A-site of the ribosome. Elongation factor-Tu forms a ternary complex with GTP and aa-tRNA, and this complex subsequently binds to the A-site of the ribosome and facilitates the growth of the polypeptide chain (Ott *et al.* 1990). Studies from different research groups suggest that EF-Tu forms protein-nucleic acid interactions with the aminoacyl end of aa-tRNAs, consisting of the T loop, T stem, aminoacyl stem and the CCA-end of tRNA (Wikman *et al.* 1982; Joshi *et al.* 1984; Metz-Boutigue *et al.* 1989). Crystal structures of the ternary complex from *Thermus aquaticus* showed that Phe-$tRNA^{Phe}$ interacts with all three domains of EF-Tu (Nissen *et al.* 1995). The 3'-CCA-Phe binds to domain II of EF-Tu in the interface between domain I and II of EF-Tu. The 5'-end and part of the acceptor stem of the aa-tRNA binds to the interfaces between the three domains and to the GTPase switch regions of the EF-Tu, where as the T stem of the tRNA binds to the surface of domain III of EF-Tu (Nissen *et al.* 1995; Nissen *et al.* 1996). Nissen and his co-workers identified residues in the switch II region (Gly 83 to Gly 94 in helix B) involved in the recognition of the major groove of the tRNA between the acceptor stem and the T stem. Residue Tyr 88, Lys 90 and Asn 91 interact with the 5'-end of the tRNA (Nissen *et al.* 1996). Based on the crystal structure of *Thermus aquaticus* EF-Tu ternary complex ((Nissen *et al.* 1995) PDB: 1TTT), Cys 81 does not directly interact with any of the

residues in the protein-nucleic acid interaction site between EF-Tu and aa-tRNA. However, Cys 81 is located in the loop connecting helix B and is about 15 Å away from both the aminoacyl ester bond at the 3'-end and the 5'-end of the aa-tRNA, suggesting that Cys 81 may have an indirect influence on aa-tRNA binding. Indeed, substitution of Cys 81 with Gly (Anborgh *et al.* 1992), Met and Ser showed reduced ability to protect aa-tRNA from spontaneously hydrolysis. Interestingly, substitution of Cys 81 to Ala resulted in similar behaviour as the wild-type (De Laurentiis *et al.* 2011). The side chain of position 81 is surrounded by residues from helix B, whose flexibility has a direct influence on the affinity for aa-tRNA (Kjaersgard *et al.* 1995), and therefore, the longer side chain of a Met at position 81 may reduce the space required for the flexibility of helix B, and may therefore limit conformational changes of the protein. This may be the reason for the reduced affinity of EF-Tu C81M for aa-tRNA. Furthermore, *Streptomyces coelicolor* and *Streptomyces ramocissimus* are the only bacteria species that have been found to have a *tuf3* gene, a low-expression *tuf* gene variant form that contains a Met at position 81(Vijgenboom *et al.* 1994; Olsthoorn-Tieleman *et al.* 2001). Interestingly, both species have a longer duplication time than *E. coli* (Cox 2004) and multiple copies of *tuf* genes of which at least one copy contains a Cysteine in position 81 (Vijgenboom *et al.* 1994). Thus, although *E. coli* EF-Tu_{MVV} showed reduced affinity to aa-tRNA, this may not be lethal for *Streptomyces* species due to the presence of *tuf* genes with Cys at position 81. On the other hand, substitution of Cys by Gly may increase the space between residue 81 and its surrounding atoms, which could potentially increase the flexibility of helix B, leading to a reduced affinity of EF-Tu for aa-tRNA. Ala has a shorter side chain than Cys, but protein variants are still able to protect aa-tRNA from

hydrolysis to an extent similar to the wild-type. Surprisingly, although Ser has a similar structure than Cys, substitution of Cys 81 with Ser significantly decreased the affinity of the protein for aa-tRNA, suggesting that more than just the size and shape of the amino acid in position 81 is important for the function of EF-Tu. Serine may affect aa-tRNA binding to EF-Tu by altering the protonation of the –OH side chain, therefore, changing the hydrogen bonding properties and the conformation of helix B.

In all living cells, the key function of EF-Tu is to transport the aa-tRNA to the A-site of the actively translating ribosome. The cognate codon-anticodon interaction triggers the hydrolysis of GTP bound to EF-Tu, and subsequent dissociation of EF-Tu·GDP from the ribosome and peptide bond formation. In this study, EF-Tu variants showed similar relative activity in the dipeptide formation as the wild-type, suggesting all three EF-Tu variants can efficiently form ternary complexes with GTP and aa-tRNA, and subsequently deliver aa-tRNA to ribosomal A-site under the assay condition (see section 3.4). Further experiments need to be carried out test if these three substitutions at position 81 affect *in vitro* poly(Phe) synthesis under multiple turnover condition.

5.1.3 Ribosome-stimulated GTPase activity

Cryo-EM and X-ray structures of EF-Tu bound to the ribosome revealed that domain I of EF-Tu is involved in the interaction with the sarcin-ricin loop (SRL) of the 23S RNA of the 50S ribosomal subunit (Stark *et al.* 2002; Voorhees *et al.* 2010). The SRL has been shown to be crucial for GTPase activation. Schuette and colleagues hypothesized that the catalytic residue His 84 of EF-Tu in the GTP-bound conformation sterically clashes with the SRL causing a rearrangement of switch II of EF-Tu which then

induces GTP hydrolysis (Schuette *et al.* 2009). Mutations C81G, G83A, H84A all showed a reduced ribosome-stimulated GTPase activity (Anborgh *et al.* 1992; Kjaersgard *et al.* 1995; Daviter *et al.* 2003), suggesting a conformational change in the switch II region of the mutants interfering with GTPase activation. In this study, all three EF-Tu variants AVV, MVV and SVV showed reduced (>three-fold) aa-tRNA independent ribosome-stimulated GTPase activity under multiple turnover conditions. This suggests that although Ala and Met are found in nature as substitutions for Cys 81, mutations may affect the conformation of the switch II region and, therefore, limit the GTPase activation in *E. coli* EF-Tu in the absence of aa-tRNA. The fact that dipeptide formation, which follows GTP-hydrolysis in the presence of aa-tRNA, seems not to be affected by the introduced substitutions indicates that under the assay condition the codon-anticodon interaction can trigger additional signals through, for example the tRNA that can compensate the effect of the Cysteine 81 mutants reported here. Therefore, further experiments can be performed to test if the presence of aa-tRNA can rescue ribosome-stimulated EF-Tu GTPase activity for all three variants.

5.2 Effect of domain II mutants on ribosome-stimulated EF-Tu's GTPase activity

Upon correct codon-anticodon recognition, local changes at the decoding center trigger a conformational change in the 30S ribosomal subunit from an open to a close conformation, where the shoulder domain of the 30S subunit moves towards the ternary complex (Ogle *et al.* 2002), which ultimately contributes to stimulating EF-Tu's GTPase activity. Although the kinetic mechanism of EF-Tu dependent aa-tRNA binding to the ribosome has been studied to great detail (Rodnina *et al.* 1995; Pape *et al.* 1998; Kothe and Rodnina 2006), the exact signalling pathway for EF-Tu's GTPase activation is

unclear. Therefore, residues in domain II of EF-Tu involved in ribosomal interactions were examined in this study.

Piepenburg and colleagues proposed two signalling pathways for ribosome-stimulated GTPase activation of EF-Tu. One is through direct contact between EF-Tu and the ribosome and another involves a conformational change in aa-tRNA, which induces a conformational change in EF-Tu. Different investigations have suggested that conformational changes in the D loop (Rodnina *et al.* 1994) and T loop of aa-tRNA (Piepenburg *et al.* 2000; Valle *et al.* 2002) may translate an interaction in the decoding center into a signal for GTPase activation in EF-Tu via S12 in the 30S subunit (Gregory *et al.* 2009). However, recent cryo-EM and X-ray crystal structure suggest that the 30S subunit not only interacts with aa-tRNA, but also with domain II of EF-Tu at residues 232-235 at helix 5 and Arg 291 in *T. thermophilus* (Arg 279 in *E. coli*) at helix 15 of 16S rRNA (Schuette *et al.* 2009; Voorhees *et al.* 2010). Interestingly, substitution of G280V on EF-Tu in *Salmonella typhimurium* (G280 in *E. coli*) (Tubulekas and Hughes 1993) and G222D in *E. coli* (Vorstenbosch *et al.* 1996) showed impaired GTPase activity, indicating the signal may also travel directly through the 16S rRNA in 30S subunit and domain II in EF-Tu.

5.2.1 Guanine nucleotide binding properties

Residues R279, G280, and R283 are located in domain II of *E. coli* EF-Tu, far away from both the nucleotide binding pocket and EF-Ts interaction site. Their locations are consistent with the results reported here that mutating them to Alanine and Glycine does not alter the nucleotide binding properties and the interaction of EF-Tu with EF-Ts.

5.2.2 Ribosome-stimulated GTPase activity and the effect of Mg^{2+} concentration

Tubulekas and colleagues demonstrated that the substituion of G280V in *Salmonella typhimurium* reduced the ability of EF-Tu to interact with ribosomes, and that the ribosome-dependent GTPase stimulation was less efficient. But no effect on nucleotide binding affinity, interaction with EF-Ts and the formation of the ternary complex were observed (Tubulekas and Hughes 1993). Interestingly, the structure of the kirromycin stalled *T. thermophilus* EF-Tu ternary complex bound to *T. thermophilus* ribosome revealed that Arg 291 (Arg 279 in *E. coli*) forms a hydrogen bond with the backbone of 16S rRNA helix 15 U367 (Schuette *et al.* 2009) and that residues 278 to 280 (in *E. coli*) interact with 16S rRNA nucleotides 367 and 368 via hydrophobic interactions (Schmeing *et al.* 2009). Although Gly 280, and Arg 283 (*E. coli*) do not directly contact the 16S rRNA, the G280V and R283A, as well as R279A variants showed reduced ribosome-stimulated GTPase activity in the EF-Tu·GTP binary complex. It also has been suggested that the 16S rRNA may undergo a conformational change upon binding to mRNA (Brock *et al.* 2008). Therefore, EF-Tu's GTPase activity was also tested in the presence of poly(U) programmed ribosomes. The GTPase activity of EF-Tu variants was not enhanced by the presence of mRNA in the ribosome, consistent with wild-type EF-Tu that did not show increased GTPase activation, suggesting that the conformational change in 16S rRNA does not alter the interaction site between EF-Tu and the rRNA. Mutations G280V and R283A may alter the conformation of the loop containing Arg 279, hence, disrupting the interaction between Arg 279 and U367 which may disrupt the signal transmission for GTPase activation.

Interestingly, it has been noticed that U368, a downstream nucleotide to U367 on 16S rRNA, together with A55 also contact residues 232-235 in domain II of EF-Tu (Schuette *et al.* 2009). Mutations on corresponding residue on *E.coli* EF-Tu G222D showed that the substitution has no effect on the initial binding of the ternary complex to the ribosome and the codon recognition. But at low Mg^{2+} concentration (5 mM), the G222D substitution inhibited the tRNA conformation change after codon recognition, subsequent GTPase activation and A-site binding. However, at higher Mg^{2+} concentration (10 mM) all activities were restored (Vorstenbosch *et al.* 1996). Previous kinetic studies suggested that Mg^{2+} is also important for GTP hydrolysis as increased GTPase activation of wild-type EF-Tu was observed with increasing Mg^{2+} concentrations (Thompson *et al.* 1981); and lowering the Mg^{2+} concentration from 10 mM to 5 mM may result in a decrease in the rate of GTP hydrolysis, which significantly improves the selectivity of aa-tRNA binding and overall translation (Pape *et al.* 1999). This is consistent with the observation that Mg^{2+} is essential for maintaining the ribosome structure and flexibility (Liiv and O'Connor 2006; Selmer *et al.* 2006; Yamamoto *et al.* 2010). Available crystal structures suggest that Mg^{2+} is important for forming intersubunit bridges between the two ribosomal subunits during translation (Selmer *et al.* 2006). To assess the role of magnesium ions on the ribosome-dependent GTPase activation of the mutant EF-Tu·GTP binary complex, different Mg^{2+} concentrations were used in ribosome-stimulated EF-Tu GTPase activity assay. Interestingly, although all EF-Tus showed lower level GTPase activation at 3 mM Mg^{2+} concentration and maximum activity at 10 mM Mg^{2+} concentration, the activities for all EF-Tu variants were lower than the wild-type control in all tested Mg^{2+} concentrations. These data suggested that increasing Mg^{2+}

concentration cannot rescue the GTPase activity of EF-Tu variants, and Mg^{2+} cannot restore the communication network between 16S rRNA and the EF-Tu by forming bridges between the two molecules.

More interestingly, kirromycin is a antibiotic that inhibit the release of EF-Tu from the ribosome by stabilize EF-Tu at a GTP-bound like state; however, it has been shown to stimulate GTP hydrolysis of EF-Tu (Wolf *et al.* 1974). In the presence of kirromycin, all three protein variants can hydrolyze GTP with the similar rate as the wild-type. These data suggest that the reduced ribosome-stimulated GTPase activity of the EF-Tu variants is not due to losing the GTPase activity in the EF-Tu, but to the lose of communication between EF-Tu and the ribosome. These data further suggest that EF-Tu R279, G280 and R283 are involved in the signaling pathway for GTPase activation. Aminoacyl-tRNA has been shown to be important for the GTPase activation signal transmission from the decoding site on the ribosome to EF-Tu (Piepenburg *et al.* 2000), therefore, it will be interesting to examine if aa-tRNA can restore the GTPase activity of EF-Tu variants in presence of the ribosome. If the activity is restored, further experiment can be carried out to test if EF-Tu undergoes conformation changes upon aa-tRNA binding or ribosomal A-site binding that facilitate the signal transmission. If the activity cannot be restored, this will further support that residues R279, G280 and R283 in domain II of EF-Tu are an important part of the communication network between the ribosome and the EF-Tu required for GTPase activation.

Based on the findings reported here, I hypothesize that after codon –anticodon recognition, the GTPase activation signal travels from the decoding center not only via the tRNA but also via 16S rRNA to EF-Tu's domain II and causes a local rearrangement

within the EF-Tu, where switch II region in domain I containing C81 may undergo a conformation change, which is important for the activation of EF-Tu's GTPase activity.

Chapter 6 Conclusion

The findings reported here provide experimental support that a Cysteine-free (Cys-less) EF-Tu can be constructed by replacing Cys 81, 136 and 254 by Ala, Val and Val respectively, and that the protein variant has the same affinity to nucleotide and aa-tRNA as the wild-type. Therefore, interaction between aa-tRNA and EF-Tu can be studied by introducing a Cysteine residue into the Cys-less EF-Tu_{AVV} background and subsequent fluorescent labelling. However, replacing Cysteine 81 affected the ribosome-stimulated EF-Tu GTPase activation in the absence of aa-tRNA, indicating EF-Tu Cys 81 may play a functional role in the GTPase activation process.

Mutations on EF-Tu R279, G280 and R283 show lower ribosome-stimulated EF-Tu GTPase activation in the absence of aa-tRNA, but are not affected in nucleotide binding affinity and kirromycin-stimulated GTPase activity. This may indicate that these residues may indirectly be involved in the signaling pathway for GTPase activation. Therefore, base on the results from the C81, R279, G280 and R283 substitutions, I hypothesize that after codon –anticodon recognition, GTPase activation signal may require the interaction between 16S rRNA with EF-Tu domain II causing a local rearrangement in EF-Tu, likely the switch II region containing C81 in domain I, and that a subsequent rearrangement is important for the activation of the GTPase activity of EF-Tu. Therefore, further detailed analysis is needed to examine the interaction between ribosome and these protein variants.

References

Abel, K., Yoder, M.D., Hilgenfeld, R., and Jurnak, F. 1996. An α to β conformational switch in EF-Tu. *Structure* **4**(10): 1153-1159.

Agrawal, R.K., Sharma, M.R., Kiel, M.C., Hirokawa, G., Booth, T.M., Spahn, C.M., Grassucci, R.A., Kaji, A., and Frank, J. 2004. Visualization of ribosome-recycling factor on the *Escherichia coli* 70S ribosome: Functional implications *PNAS* **101**(24): 8900-8905.

Anborgh, P.H., Parmeggiani, A., and Jonak, J. 1992. Site-directed mutagenesi of elongation factor Tu. The functional and structrutal role of residue Cys81. *Eur J Biochem* **208**: 251-257.

Antoun, A., Pavlov, M.Y., Andersson, K., Tenson, T., and Ehrenberg, M. 2003. The roles of initiation factor IF2 and guanosine triphosphate in initiation of protein synthesis. *EMBO J* **22**(20): 5593-5601.

Ban, N., Nissen, P., Hansen, J., Moore, P.B., and Steitz, T. 2000. The complete atomic structure of the large ribosomal subunit at 2.4 Å resolution. *Science* **289**: 905-920.

Banerjee, R., Chen, S., Dare, K., Gilreath, M., Praetorius-Ibba, M., Raina, M., Reynolds, N.M., Rogers, T., Roy, H., Yadavalli, S.S. et al. 2010. tRNA: cellular barcodes for amino acids. *FEBS Lett* **584**: 387-395.

Brock, J.E., Pourshahian, S., Giliberti, J., Limbach, P.A., and Janssen, G.R. 2008. Ribosomes bind leaderless mRNA in *Escherichia coli* through recognition of their 5'-terminal AUG. *RNA* **14**: 2159-2169.

Carter, A.P., Clemons Jr., W.M., Brodersen, D.E., Morgan-Warren, R.J., Hartsch, T., Wimberly, B.T., and Ramakrishnan, T.V. 2001. Crystal structure of an initiation factor bound to the 30S ribosomal subuni. *Science* **291**: 498-501.

Cavarelli, J. and Moras, D. 1993. Recognition of tRNA by aminoacyl-tRNA synthetases. *FASEB J* **7**: 79-86.

Chinali, G., Wolf, H., and Parmeggiani, A. 1977. Effect of kirromycin on elongation factor Tu. Location of the catalytic center for ribosome·elongation-factor-Tu GTPase activity on the elongation factor. *Eur J Biochem* **75**: 55-65.

Chiron, S., Suleau, A., and Boonefoy, N. 2005. Mitochondrial translation: elongation factor Tu is essential in fission yeast and depends on an exchange factor conserved in humans but not in budding yeast. *Genetics* **169**(1891-1901).

Cox, R.A. 2004. Quantitative relationships for specific growth rates and macromolecular compositions of *Mycobacterium tuberculosis, Streptomyces coelicolor* A3(2) and *Escherichia coli* B/r: an integrative theoretical approach. *Microbiology* **150**: 1413-1426.

Crick, F.H.C. 1966. Codon-anticodon pairing: the wobble hypothesis. *JMB* **19**: 548-555.

Dahl, L.D., Wieden, H.J., Rodnina, M.V., and Knudsen, C.R. 2006. The importance of P-loop and domain movements in EF-Tu for guanine nucleotide exchange. *JBC* **281**(30): 21139-21146.

Daviter, T., Wieden, H.J., and Rodnina, M.V. 2003. Essential role of histidine 84 in elongation factor Tu for the chemical step of GTP hydrolysis on the ribosome. *JMB* **332**: 689-699.

De Laurentiis, E.I., Mo, F., and Wieden, H.J. 2011. Construction of a fully active Cys-less elongation factor Tu: functional role of conserved Cysteine 81. *BBA-Proteins and Proteomics* 1814(5): 684-692.

Delarue, M. 1995. Aminoacyl-tRNA synthetases. *Curr Opin Struct Biol* **5**(1): 48-55.

Diaconu, M., Kothe, U., Schlunzen, F., Fischer, N., Harms, J.M., Tonevitsky, A.G., Stark, H., Rodnina, M.V. and Wahl, M. 2005. Structural basis for the function of the ribosomal L7/L12 stalk in factor binding and GTPase activation. *Cell* 12(7): 991-1004.

Donner, D., Villems, R., Liljas, A., and Kurland, C.G. 1978. Guanosinetriphosphatase activity dependent on elongation factor Tu and ribosomal protein L7/L12. *PNAS* **75**(7): 3192-3195.

Freistroffer, D.V., Pavlov, M.Y., MacDougall, J., Buckingham, R.H., and Ehrenberg, M. 1997. Release factor RF3 in *E.coli* accelerates the dissociation of release factors RF1 and RF2 from the ribosome in a GTP-dependent manner. *EMBO J* **16**: 4126-4133.

Fujiwara, T., Ito, K., Yamami, T., and Nakamura, Y. 2004. Ribosome recycling factor disassembles the post-termination ribosomal complex independent of the ribosomal translocase activity of elongation factor G. *Mol Microbiol* **53**(2): 517-528.

Gavrilova, L.P. and Spirin, A.S. 1971. Stimulation of "non-enzymic" translocation in ribosomes by p-chloromercuribenzoate. *FEBS Lett* **17**(2): 324-326.

Gilman, A.G.A. 1987. G-proteins, transducers of receptor-generated signals. *Annu Rev Biochem* **56**: 615-649.

Godefroy-Colburn, T., Wolfe, A.D., Dondon, J., Grunberg-Manago, M., Dessen, P., and Pantaloni, D. 1975. Light-scattering studies showing the effect of initiation factors on the reversible dissociation of *Escherichia coli* ribosomes. *JMB* **94**(3): 461-478.

Gregory, S.T., Carr, J.F., and Dahlberg, A.E. 2009. A signal relay between ribosomal protein S12 and elongation factor EF-Tu during decoding of mRNA. *RNA* **15**(2): 208-214.

Grigorenko, B.L., Shadrina, M.S., Collins, J.R., and Nemukhin, A.V. 2008. Mechanism of the Chemical Step for the Guanosine Triphosphate (GTP) Hydrolysis Catalyzed by Elongation Factor Tu. *BBA* **1784**: 1908-1917.

Gromadski, K.B., Wieden, H., and Rodnina, M.V. 2002. Kinetic mechanism of elongation factor Ts-catalyzed nucleotide exchange in elongation factor Tu. *Biochemistry* **41**(1): 162-169.

Guenneugues, M., Caserta, E., Brandi, L., Spurio, R., Meunier, S., Pon, C.L., Boelens, R., and Gualerzi, C.O. 2000. Mapping the fMet-tRNA^{fMet} binding site of initiation factor IF2. *EMBO J* **19**(19): 5233-5240.

Hartz, D., Binkley, J., Hollingsworth, T., and Gold, L. 1990. Domains of initiator tRNA and initiation codon crucial for initiator tRNA selection by *Escherichia coli* IF3. *Genes Dev* **4**: 1790-1800.

Hausner, T.P., Atmadja, J., and Nierhaus, K.H. 1987. Evidence that the G2661 region of 23S rRNA is located at the ribosomal binding sites of both elongation factors. *Biochimie* **69**: 911-923.

Hoagland, M.B., Stephenson, M.L., Scott, J.F., Hecht, L.I., and Zamecnik, P.C. 1958. A soluble ribonucleic acid intermediate in protein synthesis. *JBC* **231**: 241-257.

Holley, R.W., Apgar, J., Everett, G.A., Madison, J.T., Marquisee, M., Merrill, S.H., Penswick, J.R., and Zamir, A. 1965. Structure of a ribonucleic acid. *Science* **147**: 1462-1465.

Hopfield, J.J. 1974. Kinetic proofreading: a new mechanism for reducing errors in biosynthetic processes requiring high specificity. *PNAS* **71**(10): 4135-4139.

Inoue-Yokosawa, N., Ishikawa, C., and Kaziro, Y. 1974. The role of guanosine triphosphate in translocation reaction catalyzed by elongation factor G. *JBC* **249**: 4321-4323.

Janosi, L., Hara, H., Zhang, S., and Kaji, A. 1996. Ribosome recycling by ribosome recycling factor (RRF) - an important but overlooked step of protein biosynthesis. *Adv Biophys* **32**: 121-201.

Jonak, J., Petersen, T., Clarck, B.F., and Rychlik, I. 1982. *N*-Tosyl-L-phenylalanylchloromethane reacts with cysteine 81 in the molecule of elongation factor Tu from *Escherichia coli*. *FEBS Lett* **150**(2): 485-488.

Joshi, R.L., Faulhammer, H., Chapeville, F., Sprinzl, M., and Haenni, A.-L. 1984. Aminoacyl RNA domain of turnip yellow mosaic virus Val-RNA interacting with elongation factor Tu. *Nucleic Acids Res* **12**(19): 7467-7478.

Karimi, R., Pavlov, M.Y., Buckingham, R.H., and Ehrenberg, M. 1999. Novel roles for classical factors at the interface between translation termination and initiation. *Mol Cell* **3**: 601-609.

Katunin, V.I., Savelsbergh, A., Rodnina, M.V., and Wintermeyer, W. 2002. Coupling of GTP hydrolysis by elongation factor G to translocation and factor recycling on the ribosome. *Biochemistry* **41**(42): 12806-12812.

Kawashima, T., Berthet-Colominas, C., Wulff, M., Cusack, S., and Leberman, R. 1996. The structure of the Escherichia coli EF-Tu.EF-Ts complex at 2.5 A resolution. *Nature* **379**: 511-518.

Kiel, M.C., Raj, V.S., Kaji, H., and Kaji, A. 2003. Release of ribosome-bound ribosome recycling factor by elongation factor G. *JBC* **278**: 48041-48050.

Kim, Y., Ho, S.O., Gassman, N.R., Korlann, Y., Landorf, E.V., Collart, F.R., and Weiss, S. 2008. Efficient site-specific labeling of proteins via cysteines. *Bioconjug Chem* **19**(3): 786-791.

Kisselev, L.L. and Buckingham, R.H. 2000. Translational termination comes of age. *Trends Biochem Sci* **25**(11): 561-566.

Kjaersgard, I.V.H., Knudsen, C.R., and Wiborg, O. 1995. Mutation of the conserved Gly83 and Gly94 in *Escherichia coli* elongation factor Tu. *Eur J Biochem* **228**(1): 184-190.

Kjeldgaard, M., Nissen, P., Thirup, S., and Nyborg, J. 1993. The crystal structure of elongation factor Ef-Tu from *T. Aquaticus* in the GTP conformation. *Structure* **1**(1): 35-50.

Kjeldgaard, M., Nyborg, J., and Clark, B.F. 1996. The GTP binding motif: variations on a theme. *FASEB J* **10**(12): 1347-1368.

Kothe, U. and Rodnina, M.V. 2006. Delayed release of inorganic phosphate from elongation factor Tu following GTP hydrolysis on the ribosome. *Biochemistry* **45**: 12767-12774.

Krab, I.M. and Parmeggiani, A. 2002. Mechansims of EF-Tu, a pioneer GTPase. *Prog Nucleic Acid Res Mol Biol* **71**: 513-551.

Kurland, C.G. 1992. Translational accuracy and the fitness of bacteria. *Ann Rev Genetics* **26**: 29-50.

Laursen, B.S., Sorensen, H.P., Mortensen, K.K., and Sperling-Petersen, H.U. 2005. Initiation of protein synthesis in bacteria. *MMBR* **69**(1): 101-123.

Liiv, A. and O'Connor, M. 2006. Mutations in the intersubunit bridge regions of 23 S rRNA. *JBC* **281**(40): 29850-29862.

Ling, J., Reynolds, N., and Ibba, M. 2009. Aminoacyl-tRNA synthesis and translational quality control. *Annu Rev Microbiol* **63**: 61-78.

Metz-Boutigue, M.-H., Reinbolt, J., Ebel, J.-P., Ehresmann, C., and Ehresmann, B. 1989. Crosslinking of elongation factor Tu to $tRNA^{Phe}$ by *trans*-diamminedichloroplatinum (II) characterization of two crosslinking sites on EF-Tu. *FEBS Lett* **245**(1-2): 194-200.

Moazed, D., Samaha, R.R., Gualerzi, C., and Noller, H.F. 1995. Specific protection of 16 S rRNA by translational initiation factors *JMB* **248**(2): 207-495.

Nakamura, Y. and Ito, K. 2003. Making sense of mimic in translation termination. *Trends Biochem Sci* **28**(2): 99-106.

Nierhaus, K.H. 1991. The assembly of prokaryotic ribosome. *Biochimie* **73**(6): 739-755.

Nissen, P., Kjeldgaard, M., Thirup, S., Clark, B.F.C., and Nyborg, J. 1996. The ternary complex of aminoacylated tRNA and EF-Tu-GTP. Recognition of a bound and a fold. *Biochimie* **78**(11-12): 921-933.

Nissen, P., Kjeldgaard, M., Thirup, S., Polekhina, G., Reshetnikova, L., Clark, B.F.C., and Nyborg, J. 1995. Crystal structure of the ternary complex of Phe-$tRNA^{Phe}$, EF-Tu and a GTP analog. *Science* **270**(5241): 1464-1472.

Nowotny, V. and Nierhaus, K.H. 1988. Assembly of the 30S subunit from *Escherichia coli* ribosomes occurs via two assembly domains which are initiated by S4 and S7. *Biochemistry* **27**: 7051-7055.

Ogle, J.M., Murphy IV, F.V., Tarry, M.J., and Ramakrishnan, V. 2002. Selection of tRNA by the ribosome requires a transition from an open to a closed form. *Cell* **111**: 721-732.

Olsthoorn-Tieleman, L.N., Plooster, L., and Kraal, B. 2001. The variant *tuf3* gene of *Streptomyces coelicolor* A3(2) encodes a real elongation factor Tu, as shown in a novel *Streptomyces in vitro* translation system. *Eur J Biochem* **268**: 3807-3815.

Ott, G., Schiesswohl, M., Kiesewetter, S., Forster, C., Arnold, L., Erdmann, V.A., and Sprinzl, M. 1990. Ternary complexes of *Escherichia coli* aminoacyl-tRNAs with the elongation factor Tu and GTP: thermodynamic and structural studies. *BBA* **1050**(1-3): 222-225.

Pape, T., Wintermeyer, W., and Rodnina, M.V. 1998. Complete kinetic mechanism of elongation factor Tu-depedent binding of aminoacyl-tRNA to the A site of the *E. coli* ribosome. *EMBO J* **17**(24): 7490-7497.

Pape, T., Wintermeyer, W., and Rodnina, M.V. 1999. Induced fit in initial selection and proofreading of aminoacyl-tRNA on the ribosome. *EMBO J* **18**(13): 3800-3807.

Pech, M. and Nierhaus, K.H. 2008. Ribosomal peptide-bond formation. *Chem Biol* **15**: 417-419.

Peske, F., Rodnina, M.V., and Wintermeyer, W. 2005. Sequence of steps in ribosome recycling as defined by kinetic analysis. *Mol Cell* **18**: 403-412.

Petersen, H.U., Roll, T., Grunberg-Manago, M., and Clark, B.F.C. 1979. Specific interaction of initiation factor IF2 of *E. coli* with formylmethionyl-tRNA^{fMet}. *BBRC* **91**(3): 1068-1074.

Piepenburg, O., Pape, T., Pleiss, J.A., Wintermeyer, W., Uhlenbeck, O.C., and Rodnina, M.V. 2000. Intact aminoacyl-tRNA is required to trigger GTP hydrolysis by elongation factor Tu on the ribosome. *Biochemstry* **39**: 1734-1738.

Pingoud, A., Urbanke, C., Krauss, G., Peters, F., and Maass, G. 1977. Ternary complex formation between elongation factor Tu, GTP and aminoacyl-tRNA: an equilibrium study. *Eur J Biochem* **78**: 403-409.

Potapov, A.P. 1982. A stereospecific mechanism for the aminoacyl-tRNA selection at the ribosome. *FEBS Lett* **146**(1): 5-8.

Ramakrishnan, V. 2002. Ribosome structure and the mechanism of translation. *Cell* **108**: 557-572.

Rodnina, M.V., Fricke, R., Kuhn, L., and Wintermeyer, W. 1995. Codon-dependent conformational change of elongation factor Tu preceding GTP hydrolysis on the ribosome. *EMBO J* **14**(11): 2613-2619.

Rodnina, M.V., Fricke, R., and Wintermeyer, W. 1994. Transient conformational states of aminoacyl-tRNA during ribosome binding catalyzed by elongation factor Tu. *Biochemistry* **33**: 12267-12275.

Rodnina, M.V., Gromadski, K.B., Kothe, U., and Wieden, H.-J. 2005. Recognition and selection of tRNA in translation. *FEBS Lett* **579**: 938-942.

Rodnina, M.V., Savelsbergh, A., Katunin, V.I., and Wintermeyer, W. 1997. Hydrolysis of GTP by elongation factor G drives tRNA movementon the ribosome. *Nature* **385**: 37-41.

Satterthwait, A.C. and Jencks, W.P. 1974. The mechanism of the aminolysis of acetate esters. *J Am Chem Soc* **96**: 7018-7031.

Schmeing, T.M., Voorhees, R.M., Kelley, A.C., Gao, Y.-G., Murphy IV, F.V., Weir, J.R., and Ramakrishnan, V. 2009. The crystal structure of the ribosome bound to EF-Tu and aminoacyl-tRNA. *Science* **326**(5953): 688-694.

Schuette, J.-C., Murphy IV, F.V., Kelley, A.C., Weir, J.R., Giesebrecht, J., Connell, S.R., Loerke, J., Mielke, T., Zhang, W., Penczek, P.A., Ramakrishnan, V., and Spahn, C.M. 2009. GTPase activation of elongation factor EF-Tu by the ribosome during decoding. *EMBO J* **28**(6): 755-765.

Selmer, M., Dunham, C.M., Murphy IV, F.V., Weixlbaumer, A., Petry, S., Kelley, A.C., Weir, J.R., and Ramakrishnan, V. 2006. Structure of the 70 S ribosome complexed with mRNA and tRNA. *Science* **313**: 1935-1942.

Shapiro, M.B., Merril, C.R., Bradley, D.F., Mosimann, J.E., and Holley, R.W. 1965. Reconstruction of protein and nucleic acid sequences: Alanine transfer ribonucleic acid. *Science* **150**: 918-921.

Shine, J. and Dalgarno, L. 1974. The 3'-terminal sequence of *Escherichia coli* 16S ribosomal RNA: complementarity to nonsense triplets and ribosome binding sites. *PNAS* **71**(4): 1342-1346.

Shulman, R.G., Hilbers, C.W., and Miller, D.L. 1974. Nuclear magnetic resonance studies of protein-RNA interactions: I. The elongation factor Tu.GTP aminoacyl-tRNA complex. *JMB* **90**(3): 601-607.

Song, H., Parsons, M.R., Rowsell, S., Lenonard, G., and Phillips, S.E.V. 1999. Crystal structure of intact Elongation Factor EF-Tu from *Escherichia coli* in GDP conformation at 2.05A Resolution. *JMB* **285**: 1245-1256.

Spierer, P., Wang, C.-C., Marsh, T.L., and Zimmerman, R.A. 1979. Cooperative interactions among protein and RNA components of the 50S ribosomal subunit of *Escherichia coli*. *Nucleic Acids Res* **6**(4): 1669-1682.

Srivastava, A.K. and Schlessinger, D. 1990. Mechanism and regulation of bacterial ribosomal RNA processing. *Annu Rev Microbiol* **44**: 105-129.

Stark, H., Rodnina, M.V., Wieden, H.-J., Zemlin, F., Wintermeyer, W., and van Heel, M. 2002. Ribosome interactions of aminoacyl-tRNA and elongation factor Tu in the codon-recognition complex. *Nat Struct Biol*. **9**(11): 849-854.

Sundari, R.M., Stringer, E.A., Schulman, L.H., and Maitra, U. 1976. Interaction of bacterial initiation factor 2 with initiator tRNA. *JBC* **251**(11): 3338-3345.

Sussman, J.L., Holbrook, S.R., Warrant, R.W., Church, G.M., and Kim, S.H. 1978. Crystal structure of yeast phenylalanine transfer RNA : I. Crystallographic refinement. *JMB* **123**(4): 607-630.

Thompson, R.C., Dix, D.B., Gerson, R.B., and Karim, A.M. 1981. Effect of Mg^{2+} concentration, polyamines, streptomycin, and mutations in ribosomal proteins on the accuracy of the two-step selection of aminoacyl-tRNAs in protein biosynthesis. *JBC* **256**(13): 6676-6681.

Thompson, R.C., Dix, D.B., and Karin, A.M. 1986. The reaction of ribosomes with elongation factor Tu·GTP complexes. *JBC* **261**(11): 4868-4874.

Tomsic, J., Vitali, L.A., Daviter, T., Savelsbergh, A., Spurio, R., Striebeck, P., Wintermeyer, W., Rodnina, M.V., and Gualerzi, C.O. 2000. Late events of translation initiation in bacteria: a kinetic analysis. *EMBO J* **19**(9): 2127-2136.

Trabuco, L.G., Schreiner, E., Eargle, J., Cornish, P., Ha, T., Luthey-Schulten, Z., and Schulten, K. 2010. The role of L1 stalk-tRNA interaction in the ribosome elongation cycle. *JMB* **402**: 741-760.

Tubulekas, I. and Hughes, D. 1993. A single amino acid substitution in elongation factor Tu disrupts interaction between the ternary complex and the ribosome. *Bacteriol J* **175**(1): 240-250.

Valle, M., Sengupta, J., Swami, N.K., Grassucci, R.A., Burkhardt, N., Nierhaus, K.H., Agrawal, R., and Frank, J. 2002. Cryo-EM reveals an active role for aminoacyl-tRNA in the accommodation process. *EMBO J* **21**(13): 3557-3567.

Varshney, U., Lee, C.P., and RajBhandary, U.L. 1993. From elongator tRNA to initiator tRNA. *PNAS* **90**: 2305-2309.

Varshney, U. and RajBhandary, U.L. 1992. Role of methionine and formylation of initiator tRNA in initiation of protein synthesis in *Escherichia coli*. *J Bacteriol* **174**(23): 7819-7826.

Vijgenboom, E., Woudt, L.P., Heinstra, P.W.H., Rietveld, K., van Harrlem, J., van Wezel, G.P., Shochat, S., and Bosch, L. 1994. Three tuf-like genes in the kirromycin producer *Streptomyces ramocissimus*. *Microbiology* **140**: 983-998.

Villa, E., Sengupta, J., Trabuco, L.G., Lebarron, J., Baxter, W.T., Shaikh, T.R., Grassucci, R.A., Nissen, P., Ehrenberg, M., Schulten, K. et al. 2009. Ribosome-induced changes in elongation factor Tu conformation control GTP hydrolysis. *PNAS* **106**(4): 1063-1068.

Voorhees, R.M., Scheming, T.M., Kelley, A.C., and Ramakrishnan, V. 2010. The mechanism for actication of GTP hydrolysis on the ribosome. *Science* **330**(6005): 835-838.

Vorstenbosch, E., Pape, T., Rodnina, M.V., Kraal, B., and Wintermeyer, W. 1996. The G222D mutation in elongation factor Tu inhibits the codon-induced conformatinal changes leading to GTPase activation on the ribosome. *EMBO J* **15**(23): 6766-6774.

Wieden, H.J., K.B., G., Rodnin, D., and Rodnina, M.V. 2002. Mechanism of elongation factor (EF)-Ts-catalyzed nucleotide exchange in EF-Tu contribution of contacts at the guanine base. *JBC* **277**(8): 6032-6036.

Wieden, H.J., Mercier, E., Gray, J., Steed, B., and Yawney, D. 2010. A combined molecular dynamics and rapid kinetics approach to identify conserved three-dimersional communication networks in elongation factor Tu. *Biophysical J* **99**: 3735-3743.

Wikman, F.P., Siboska, G.E., Petersen, H.U., and Clark, B.F.C. 1982. The site of interaction of aminoacyl-tRNA with elongation factor Tu. *EMBO J* **1**(9): 1095-1100.

Wolf, H., Chinali, G., and Parmeggiani, A. 1974. Kirromycin ,an inhibitor of protein biosynthesis that acts on elongation factor Tu. *PNAS* **71**(12): 4910-4914.

Wolf, H., Chinali, G., and Parmeggiani, A. 1977. Mechanism of the inhibition of protein synthesis by kirromycin. Role of elongation factor Tu and ribosomes. *Eur J Biochem* **75**: 67-75.

Yamamoto, T., Shimizu, Y., Ueda, T., and Shiro, Y. 2010. Mg^{2+} dependence of 70 S ribosomal protein flexibility revealed by hydrogen/deuterium exchange and mass spectrometry. *JBC* **285**(8): 5646-5652.

Yokosawa, H., Kawakita, M., Arai, K.-i., Inoue-Yokosawa, N., and Kaziro, Y. 1975. Binding of aminoacyl-tRNA to ribosomes promoted by elongation factor Tu. Further studies on the role of GTP hydrolysis. *JB* **77**(4): 719-728.

Young, R.Y. and Bremer, H. 1976. Polypeptide-chain-elongation rate in *Escherichia coli* B/r as a function of growth rate. *Biochem J* **160**: 185-194.

Yusupova, G.Z., Yusupov, M.M., Cate, J.H.D., and Noller, H.F. 2001. The path of messenger RNA through the ribosome. *Cell* **106**: 233-241.